The minor pilin TcpB is located at the tip of the toxin co-regulated pilus of *Vibrio cholerae* and is the receptor for the filamentous phage CTXφ

By

Miguel A. Gutierrez Rodarte

B.Sc., Colorado State University, 2014

Thesis Submitted in Partial Fulfillment of the

Requirements for the Degree of

Master of Science

in the

Department of Molecular Biology and Biochemistry

Faculty of Science

© Miguel Gutierrez 2017

SIMON FRASER UNIVERSITY

Summer 2017

All rights reserved.

However, in accordance with the Copyright Act of Canada, this work may be reproduce, without authorization, under the conditions for “Fair Dealing.” Therefore, limited reproduction of this work for the purposes of private study, research, criticism, review and news reporting is likely to be in accordance with the law, particularly if cited appropriately.

Approval

Name:	**Miguel A. Gutierrez Rodarte**
Degree:	**Master of Science**
	(Molecular Biology and Biochemistry)
Title:	**The minor pilin TcpB is located at the tip of the toxin co-regulated pilus of *Vibrio cholerae* and is the receptor for the filamentous phage CTXφ**

Examining Committee:

Chair: Dr. Fiona Brinkman
Professor

Dr. Lisa Craig
Senior Supervisor
Professor

Dr. Jamie K. Scott
Supervisor
Professor

Dr. Carl Lowenberger
Supervisor
Professor
Department of Biological Sciences

Dr. Ralph Pantophlet
Internal Examiner
Associate Professor
Faculty of Health Sciences

Date Defended/Approved: July 19th, 2017

Abstract

Type IV pili are polymers of the major pilin subunit found on the surfaces of many Gram-negative bacteria. They act like grappling hooks, undergoing cycles of polymerization, adhesion, and retraction, to mediate a diverse array of functions, including twitching motility, DNA uptake and adhesion. T4P possess several minor pilins, which are homologous to the major pilin but are produced in much lower quantities. Minor pilins prime Type IV pili assembly and have been proposed to localize to the tip of the pilus, but this has not been shown definitively. The *Vibrio cholerae* toxin co-regulated pilus (TCP) is a T4P that mediates microcolony formation, which is critical for the development of the gastrointestinal disease cholera. TCP is the primary receptor for the filamentous cholera toxin phage CTXφ, which binds to the pilus via its tip-associated protein, pIII. TCP possess a single minor pilin, TcpB, which initiates pilus assembly as well as retraction. We hypothesized that TcpB is located at the tip of the pilus and forms the binding site for CTXφ pIII. Here I use direct and competition ELISA to show that recombinantly expressed soluble TcpB and pIII interact. I show that CTXφ phage infection of *V. cholerae* is reduced 90 % in the presence of soluble TcpB or anti-TcpB antibody. Furthermore, gold-labeled anti-TcpB antibody binds to the tip of purified TCP, providing the first direct localization of a minor pilin to the tip of a T4P. Finally, I show that phage uptake is reduced 98 % in a retraction-deficient *V. cholerae* strain, demonstrating the role of pilus retraction in this process. My results define a two-step mechanism for CTXφ infection of *V. cholerae*, which involves (i) binding of CTXϕ via its tip-associated pIII protein to its receptor, TcpB, at the tip of the pilus, and (ii) retraction of the pilus, which pulls CTXφ into the bacterial periplasm as if it were an extension of the pilus.

Keywords:
Type IV pili; Vibrio cholerae; Toxin co-regulated pili; Cholera toxin bacteriophage; Minor pilin

Dedication

To my family for their unconditional love and support.

To Carlos Jaimes and Julie Noriega for their generosity and friendship.

To Peter Fleming for his support, guidance and encouragement.

Acknowledgements

The work completed here would not have been possible without the guidance and support of my mentors, colleagues, friends, and family. I would like to thank my senior supervisor Dr. Lisa Craig who gave me the opportunity to learn and grow under her mentorship. And for her constant support and guidance. Dr. Craig's innate ability to motivate students even when the science seems ambiguous and her capability to dissect and explain difficult concepts are qualities that I admire and I hope to emulate in my scientific career.

I would like to thank my colleagues in the Craig lab for creating an engaging and supportive atmosphere to work in. I would like to thank Dr. Subramania Kolappan, Tony Harn and Dr. Dixon Ng for their mentorship and guidance, Navi Garcha, Tuba Altindal and Bailey Burrell for their support and friendship. I would like to thank Dr. Li Yang for TEM training, Dr. Naveed Gulzar for his guidance on ELISA experiments.

I have had the opportunity to work with a group of talented undergraduate students in the lab who have collectively contributed to the work and effective functioning of the laboratory including: Shayda Swann, Matthew Chung and Brenden Westen.

Last but not least, I would like to thank Elle Killingsworth for always supporting my decisions and choices and providing me with unconditional love and support throughout my graduate journey.

The work in this thesis project was made possible by grant funding from the Canadian Institutes of Health Research.

Table of Contents

List of Tables

List of Figures

List of Acronyms

AA	Autoagglutination
Abs	Absorbance
Amp	Ampicillin
$AmSO_4$	Ammonium sulfate
AP	Alkaline phosphatase
BAM	β-barrel assembly machinery
BSA	Bovine serum albumin
BACTH	Bacterial two-hybrid system
cAMP	Cyclic adenosine monophosphate
CT	Cholera toxin
CTXΦ	Cholera toxin phage CTX-phi
DNA	Deoxyribonucleic acid
EDTA	Ethylenediaminetetraacetic acid
ELISA	Enzyme-linked immunosorbent assay
ETEC	Enterotoxigenic Escherichia coli
HRP	Horseradish peroxidase
IMCP	Inner membrane core protein
IPTG	Isopropyl β-D-thiogalactopyranoside
Km	Kanamycin
LB	Lysogeny broth
LCR	Low complexity region
M	Molar concentration

OD	Optical density
PAGE	Polyacrylamide gel electrophoresis
PBS	Phosphate buffered saline
pH	Potential of hydrogen
pNPP	para-nitrophenylphosphate
PVDF	Polyvinylidene difluoride
Rh	Rhamnose
RT	Room temperature
Sm	Streptomycin
SUP	Filtered culture supernatant
T2S	Type II secretion
T4P	Type IV pili/pilus
T4a	Type IVa pili/pilus
T4b	Type IVb pili/pilus
TBST	Tris-buffered saline with 0.1% Tween
TCP	Toxin co-regulated pilus
TEM	Transmission electron microscopy
UA	Uranyl acetate
UNICEF	United Nations Children's Fund
VPI	*Vibrio* pathogenicity island
WC	Whole cell
WT	Wild type

Chapter 1. General introduction

Gram-negative bacteria are characterized by their cell envelopes composed of an inner and outer lipid membrane with a periplasmic space in between containing a thin layer of peptidoglycan. Gram-negative bacteria comprise a wide variety of non-pathogenic and pathogenic bacteria including *Pseudomonas aeruginosa, Escherichia coli, Vibrio cholerae, Neisseria meningitidis, N. gonorrhoeae,* which can cause illnesses such as pneumonia, gastroenteritis, meningitis, bloodstream infections, sexually transmitted diseases, wound or surgical site infections and others. Given the global implications these bacterial pathogens have on health and economics, there is great interest in understanding their molecular mechanism of pathogenesis to improve upon existing therapeutics and diagnostic assays.

Gram-negative bacteria infections can be particularly difficult to treat due the double membrane nature of their cell envelope which includes an outer membrane that is absent in Gram-positive bacteria. The main function of the outer membrane is to serve as a permeability barrier but it also acts as an additional protective barrier, protecting the cells from harmful chemicals in their environment, including certain drugs and antibiotics from penetrating the cell (Silhavy et al., 2010). The most common type of antibiotics are β-lactams which function by inhibiting cell wall synthesis. More specifically, β-lactam antibiotics block steps in the biosynthesis of peptidoglycan and make cells prone to osmotic lysis. Gram-negative bacteria are less susceptible to β-lactams, which can be blocked by the outer membrane. Additionally, bacteria can develop resistance to β-lactams by employing a variety of mechanisms including

production of enzymes that break down the β-lactam ring and active expulsion of β-lactam molecules via efflux pumps (Wilke et al., 2005). According to the World Health Organization, certain types of Gram-negative bacteria are becoming increasingly resistant to available antibiotic drugs and treatments. And bacteria such as *Acinetobacter, Pseudomonas* and various Enterobacteriaceae fall into the critical category of “priority pathogens” in urgent need for novel antibiotics (WHO, 2017). The antimicrobial resistance problem represents one of the greatest threats to human health, resulting in increased illness and death from bacterial infections, and escalating healthcare costs (WHO, 2017).

Due the increased threat of antimicrobial resistance, it is clear that there is an increased need to develop new strategies to combat bacterial infections. Thus, for my thesis project I have investigated a bacterial transport system, the Type IV pilus, which is capable of actively exporting bacterial proteins and taking up specific substances. The Type IV pilus has the potential to be used as a highly efficient and specific delivery pathway for antimicrobial compounds, which would involve specific binding and uptake into the periplasm of Gram-negative bacteria. In my project, I used *V. cholerae* as a model organism to explore this concept.

1.1. *Vibrio cholerae*

V. cholerae are curved rod shaped Gram-negative bacteria (Figure 1-1) that cause the severe gastrointestinal disease cholera (Kaper et al., 1995). Cholera disease is contracted by ingestion of food or water contaminated with high concentrations of *V. cholerae*. These bacteria colonize the epithelial lining of the small intestine and secrete cholera toxin, resulting in profuse watery diarrhea that, if untreated, can rapidly lead to fatal dehydration. Cholera is a major public health problem in developing countries where clean water and sanitation facilities are inadequate. Cholera is a pandemic disease and one of the most prevalent water-related diseases in many regions of the world, particularly in South Asia, sub-Saharan Africa, and Latin America. According to the World Health Organization there are 3 to 5 million people affected and over 100,000 deaths occur every year due to this illness. Additionally, cholera outbreaks occur in other parts of the world, typically in regions that have been destabilized by war or natural disasters. Such is the case for the cholera outbreak in Haiti that followed the major earthquake in 2010 and continues to this day. More than 70,000 cases of cholera were reported and over 8000 deaths were caused by the disease (WHO, 2015). A cholera outbreak in Yemen, which is in the middle of a civil war, was first reported during April 2017 and has been expanding at an alarming rate, with roughly 70,000 cases reported over the first month (WHO, 2017). And according to the UNICEF regional director for the Middle East and North Africa, the number of cholera cases could reach 300,000 in the war-ravaged country within the next month. The main reservoirs of *V. cholerae* are aquatic sources that are somewhat salty and warm such as estuaries and some coastal areas, as well as humans. Recent studies indicate that

climate change is creating an increasingly more favorable environment for *V. cholerae*, which will likely increase its disease burden (Vezzulli et al., 2016).

V. cholerae are classified on the basis of the O antigen of lipopolysaccharide (LPS) which are molecules composed of lipid and polysaccharide that form the outer leaflet of the outer membrane of Gram-negative bacteria. LPS is critical for structural integrity of the membrane and is a potent endotoxin. Over 200 different *V. cholerae* serogroups have been identified to date, differing in the chemistry of their O antigen. Most of these are harmless aquatic microbes and the majority of pathogenic serogroups cause only mild gastroenteritis (Kaper et al., 1995). Two *V. cholerae* serogroups – O1 and O139 – cause pandemic cholera. Within the O1 serogroup there are two biotypes: classical and El Tor. The classical biotype was responsible for six of the seven recorded cholera pandemics, and the El Tor biotype is responsible for the on-going seventh pandemic (Kaper et al., 1995).

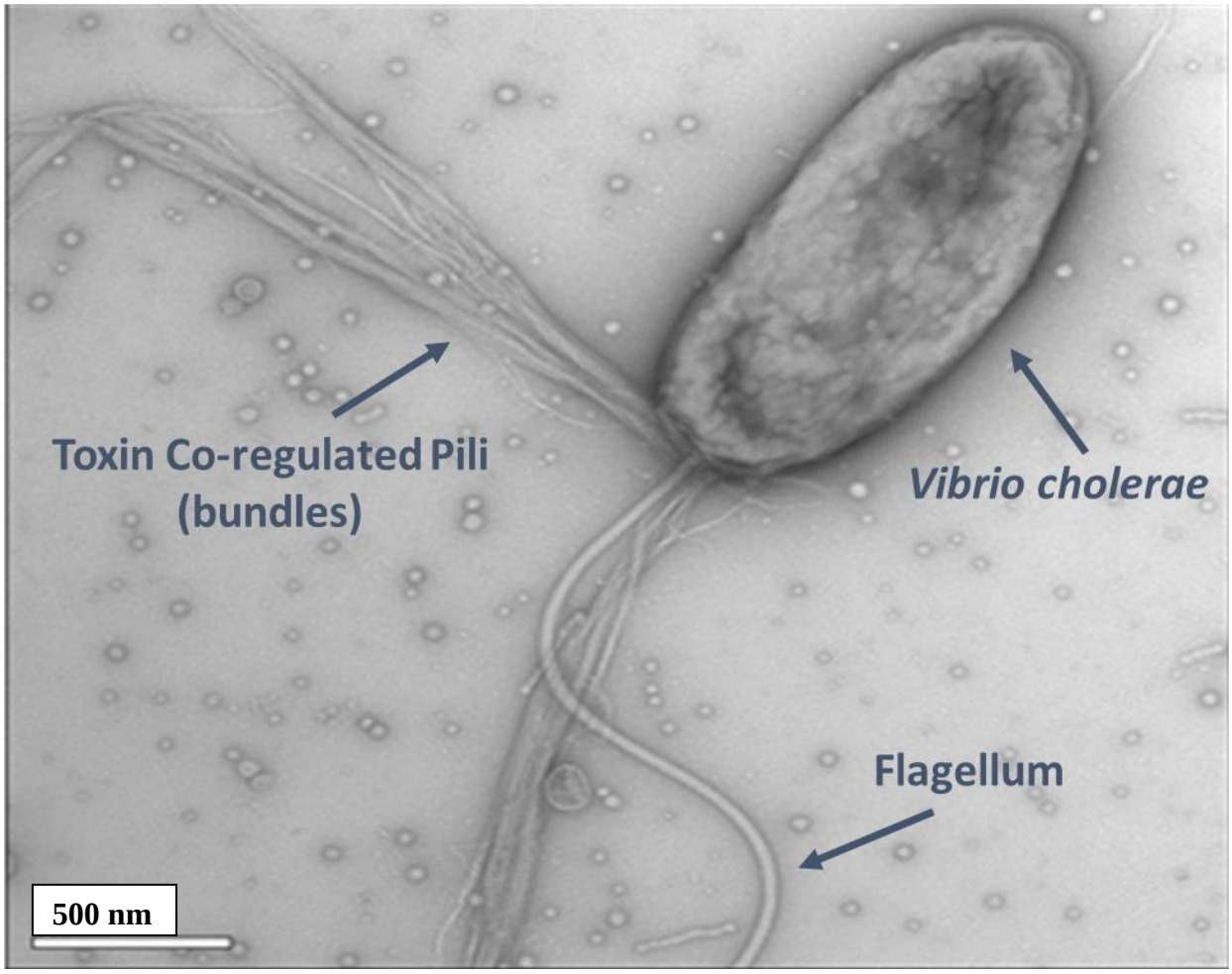

Figure 1-1. Transmission electron micrograph (TEM) of a *Vibrio cholerae* cell. Rod-shaped, Gram-negative *V. cholerae* cell expressing toxin co-regulated pilus filaments in bundles with their polar flagella found on the end of the bacterium. *V. cholerae* wild type strain O395 grown in pilus-inducing conditions and stained with 3% uranyl acetate. Imaging done on Hitachi 8100 Scanning TEM by Lisa Craig.

1.2. Vibrio cholerae pathogenesis

Cholera disease starts with the oral ingestion of food or water contaminated with *V. cholerae*. The bacteria must survive passage through the gastric acid barrier of the stomach, then penetrate the mucus lining that coats the epithelia of the small intestine to bind to epithelial cells (Fig. 1-2). Binding triggers the expression of virulence factors cholera toxin and toxin coregulated pili which facilitate micro-colony formation via pilus to pilus interactions (Craig et al. 2004; DiRita et al., 1991). Once colonization has occurred, *V. cholerae* secrete cholera toxin via the type II secretion system (Davis et al., 2000). Cholera toxin is responsible for disturbing the water-electrolyte balance in the intestinal epithelium at a cellular level, resulting in the profuse watery diarrhea that is characteristic of the cholera disease. Cholera toxin is taken up into the epithelial cells via monosialogangliosides on GM1 receptors. Once within the cell, cholera toxin activates the adenylate cyclase-cAMP system located at the basolateral membrane of intestinal epithelial cells which results in a massive efflux of water and electrolytes from the cell (DiRita et al., 1991). The extreme diarrhea and dehydration cause decreased intravascular volume, hypotension and hypoperfusion of critical organs leading to systemic shock. The rate of body fluid loss is greatest in the jejunum with up to 20 liters lost per day in adults. In such severe cases death can follow within 12 hours of appearance of the first symptoms (Levine et al., 1983).

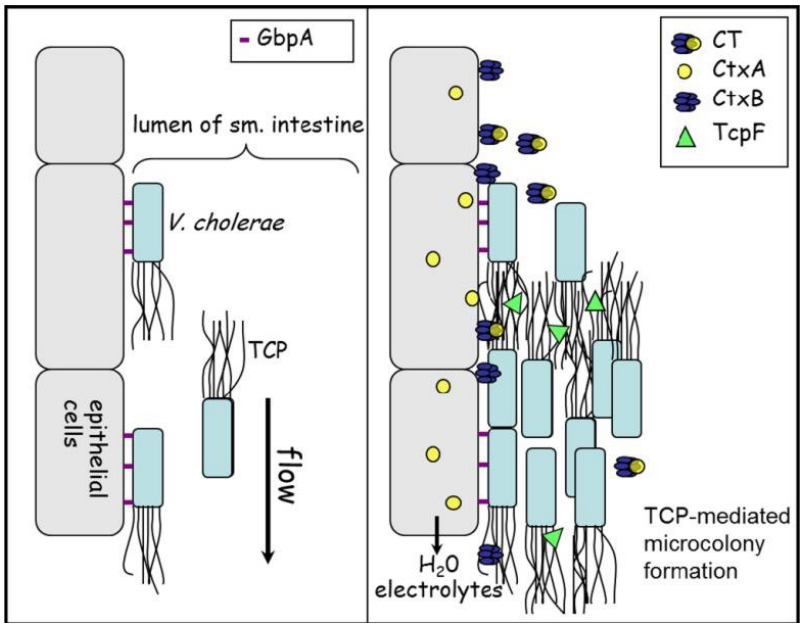

Figure 1-2. *V. cholerae* colonization of epithelial cells, TCP-mediated microcolony formation.
Upon entry into the host, *V. cholerae* attach to intestinal epithelial cells. The bacteria adhere to the small intestine through TCP and adhesins which leads to microcolony formation. Cholera toxin is synthesized and secreted upon adhering to the epithelial cells. Uptake of the toxin results in massive loss of water and electrolytes, resulting in severe diarrhea (Kaper et al., 1995). Image courtesy of L. Craig, Simon Fraser University.

1.1.3. Cholera toxin

Cholera toxin is an ADP-ribosylating, AB5–subunit type toxin. It is made up of a large catalytic A subunit bound to a pentamer of 5 binding B subunits (Lonnroth and Holmgren 1973; Lospalluto and Finkelstein, 1972). The B subunit is responsible for binding to receptors and allowing the A subunit to enter the cell where it highjacks the host cell's regular functions. The cholera toxin pathogenic mechanism begins when the pentameric B subunit interacts with the high-affinity monosialoganglioside GM1 receptors on the surface of intestinal mucosal cells (van Heyningen, 1976). Endocytosis of cholera toxin may occur via lipid raft/caveolae mediated endocytic pathway, clathrin mediated endocytic pathway, or the ADP-ribosylation factor 6-associated endocytic pathway. Cholera toxin is transported to the endoplasmic reticulum in a retrograde fashion where the A subunit is hydrolyzed, releasing it from the B pentamer in a catalytically active form, A1. The A1 domain is an ADP-ribosylase that targets the alpha subunit of the G_s protein, a guanine nucleotide binding regulator protein. ADP-ribosylation of the G_s protein leads to its constitutive activation of adenylate cyclase, a substrate of G_S, which elevates levels of cyclic-AMP (cAMP). The high levels of cAMP activate cAMP-dependent protein kinase A (PKA), which phosphorylates the cystic fibrosis transmembrane conductance regulator chloride ion channels (Bubien et al., 1994; Field, 1977; Goodman and Percy, 2005; Levistre et al., 1995). Phosphorylation opens the channels, resulting in a rapid efflux of water and electrolytes, causing severe watery diarrhea with the “rice water stool” that is characteristic of cholera disease (Fig. 1-3).

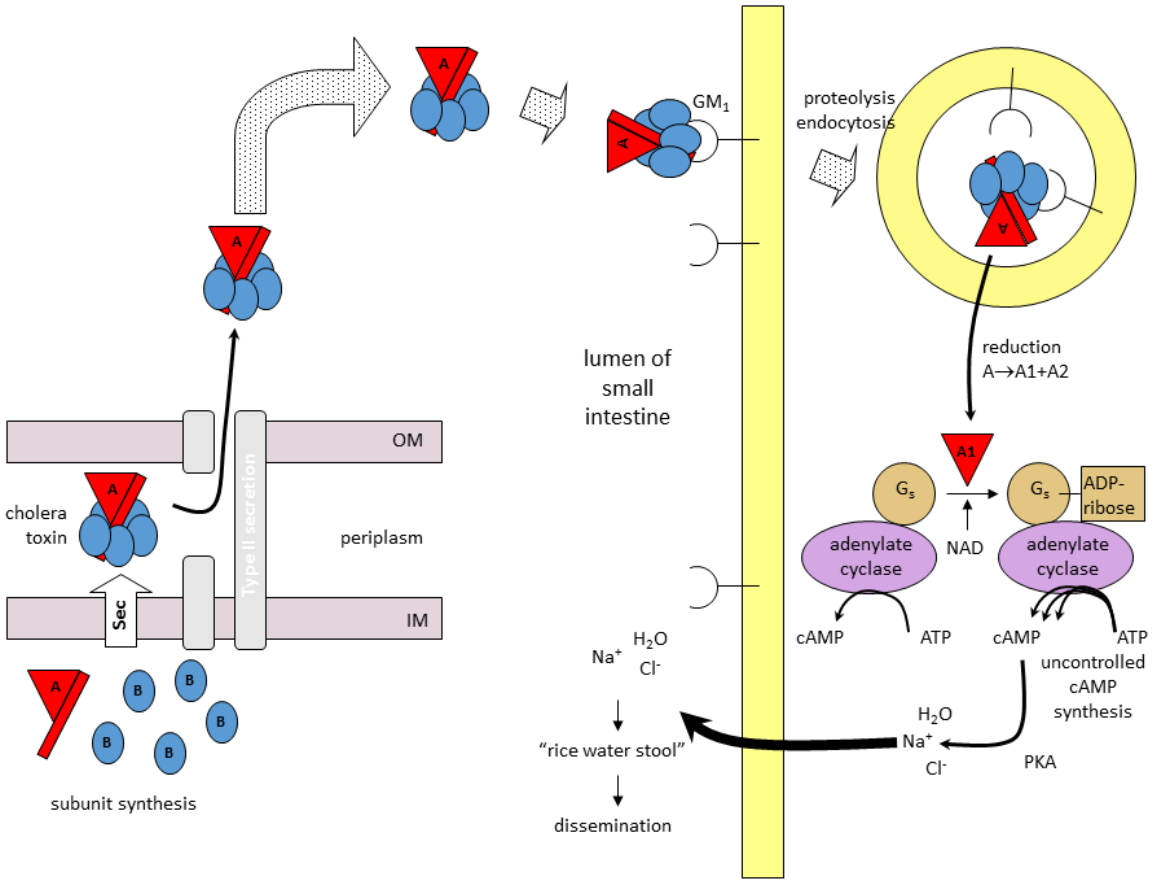

Figure 1-3 Cholera toxin mechanism. Cholera toxin is an AB5 toxin that is secreted by the type II secretion system of *V. cholerae*. The pentameric B subunit binds to the GM1 ganglioside of intestinal epithelial cells and this causes endocytosis of the A subunit which consequently becomes activated in the reducing conditions of the cell. The activated A1 subunit ADP-ribosylates the G protein which targets adenylate cyclase, resulting in uncontrolled cAMP signaling, electrolyte imbalance and water secretion (Kaper et al., 1995; Lemichez and Stefani, 2013). Image courtesy of Lisa Craig, Simon Fraser University.

1.1.4. Genetic elements of virulence

The two key virulence factors for *V. cholera* pathogenesis are the toxin coregulated pilus (TCP) and cholera toxin, which are encoded on two gene clusters: the *Vibrio* pathogenicity island (VPI-1) encoding the *tcp* operon and the CTX element, which is a prophage encoding phage proteins and cholera toxin (Waldor and Mekalanos, 1996; Craig et al., 2004; Pearson et al., 1993). The acquisition of these mobile genetic elements of virulence is responsible for the conversion of non-pathogenic marine *V. cholerae* to pathogenic biotypes. Only strains containing both of these genetic elements cause epidemic cholera (Taylor et al., 1987).

1.1.4.1 Vibrio pathogenicity island (VPI-1)

The *V. cholerae* pathogenicity island 1 (VPI-1), located on chromosome I, is considered to be the most important genomic island involved in the evolution of pathogenic *V. cholerae* strains. This VPI is 41.2 kb in size in and encodes 29 potential proteins (Karaolis et al., 1998). VPI-1 encodes proteins with essential roles in virulence, such as proteins that regulate expression of both TCP and cholera toxin, such as the transcription activators ToxT, TcpP and TcpH. (Carroll et al., 1997; DiRita et al., 1991; DiRita, 1992; Häse and Mekalanos, 1998).

TCP is called the “toxin coregulated pilus” because its expression is coordinated with expression of cholera toxin by a regulatory system consisting of three different transcriptional activators, ToxT and TcpP, and ToxR. (Karaolis et al.,

1998; Kovach et al., 1996). The transcriptional activator ToxT directly activates expression of both the *ctx* and *tcp* gene clusters, as well as additional genes. *V. cholerae* strains lacking ToxT make no cholera toxin or TCP and are non-pathogenic (Champion et al., 1997). The microbial origins of VPI-1 are not known.

1.1.4.2 CTX element

The cholera toxin genes were acquired by *V. cholerae* via the filamentous bacteriophage CTXφ (Waldor and Mekalanos, 1996), which binds to the toxin coregulated pilus (Kirn et al., 2000; Waldor and Mekalanos, 1996) and is taken up by the bacterium. The CTXφ phage genome becomes integrated into the *V. cholerae* chromosome I (Waldor and Mekalanos, 1996). The CTXφ genome is integrated site-specifically at the homologous region attRS1 of *V. cholerae* chromosome 1, as a tandem prophage. The genome of CTXφ contains a central core region with a repetitive sequence (RS), designated RS2, which integrates site-specifically at attRS1 (Fig. 1-4) (Basu et al., 2000; Pearson et al., 1993). The CTX element core region encodes the phage assembly proteins and the cholera toxin subunits A and B; the repetitive sequences are involved in site-specific recombination of the CTXφ genome. The RS2 region is located upstream of the CTX element central core and contains three open reading frames that encode proteins involved in the regulation (*rstR*), replication (*rstA*) and integration (*rstB*) of CTXφ genome.

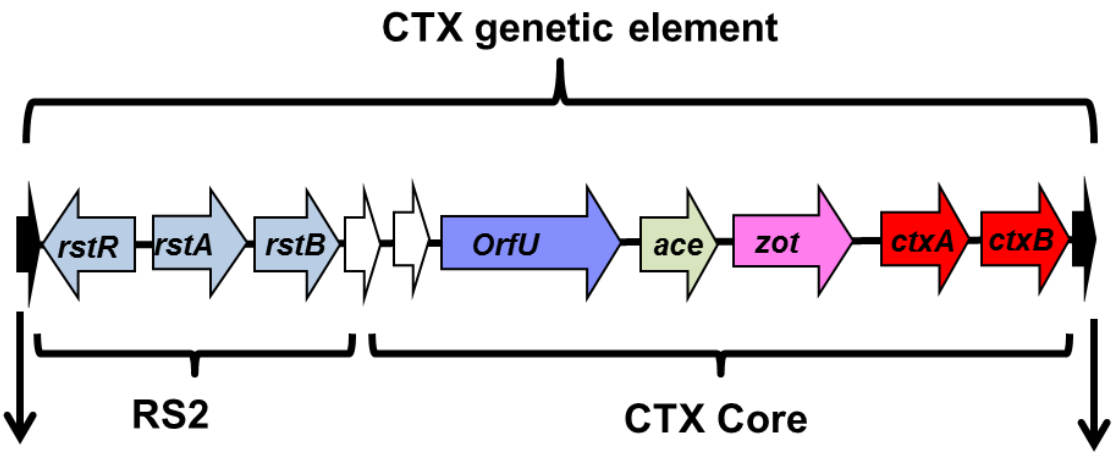

Figure 1-4. Diagram of the arrangement of the CTX genetic element within the *V. cholerae* genome. CTX genetic element includes RS2 and the CTX core. The CTX element can be flanked by one or more copies of RS1(not shown). Open reading frames are shown as arrows. The black triangles represent CTXφ attachment sites (attRS).

1.1.5 Evolution of pathogenic *V. cholerae*

Cholera is an ancient disease, having been reported for centuries. During the 19th century, *V. cholerae* spread across the world from its original reservoir in the Ganges Delta in India. There have been seven recorded pandemics of cholera, beginning in 1817, which have killed millions of people across all continents. The current, seventh pandemic started in South Asia in 1961, reached Africa in 1971 and the Americas in 1991 (Dziejman et al., 2002; Pollitzer et al., 1959).

The *V. cholerae* benign marine bacterium evolved into a dangerous human pathogen, likely hundreds or thousands of years ago by the acquisition of the transmissible elements VPI, and phage CTXφ. The TCP is the receptor for CTXφ. Once *V. cholerae* acquired the VPI and expresses the TCP, it became susceptible to CTXφ transduction.

The acquisition of CTXφ genome was a central event in the emergence of *V. cholerae* as a pathogen. The source of the *ctxAB* genes within the CTXφ genome is not known. The acquisition of *ctxAB* genes by the progenitor of CTXφ, pre-CTXφ, increased its fitness since CTXφ confers a selective advantage to the *V. cholerae* host by allowing it to produce cholera toxin; the profuse diarrhea that results from this enterotoxin promotes dissemination of the bacterium and hence the phage. CTXφ forms stable lysogens in *V. cholerae,* allowing propogation of the phage genome with each bacterial division, and replication of the phage does not cause *V. cholerae* cell lysis.

The similarity between pathogenic O139 serogroup and the El Tor biotype of the O1 serogroup indicates that epidemic O139 strains are derived from O1 El Tor strains (Fig. 5) (Berche et al., 1994; Higa et al., 1993; Waldor et al., 1994). This

new O139 variant was able to circumvent established immunity in human populations that had been previously exposed to O1, and resulted in large outbreaks in 1992 in Bangladesh and India.

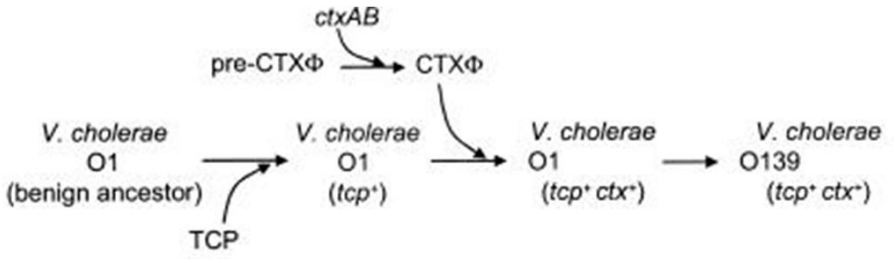

Figure 1-5. Evolution of pathogenic *V. cholerae*. CTXφ was acquired by a TCP expressing O1 strain after it diverged from a benign ancestor.

1.2. The filamentous phage CTXφ

CTXφ is the filamentous bacteriophage specific for *V. cholerae*. It was first identified in 1996 and it was the first filamentous phage to be shown to horizontally transmit a virulence factor via lysogenic conversion to a pathogenic bacterium, conferring *V. cholerae* with the ability to produce cholera toxin (Waldor and Mekalanos, 1996; Lencer and Tsai, 2003; Ochman et al., 2000).

1.2.1. Homology of CTXφ and Ff family (M13, fd, f1) phage

The CTXφ genome is very similar in structure and gene organization to that of the *E. coli* filamentous coliphage of the Ff family (M13, fd, f1) (Fig. 1-6), though sequence similarity among these genomes is low (Pollastri and McLysaght, 2005). In fact, much of what is known about CTXφ was first extrapolated by comparison to the Ff family. The structure, genetics and mechanism of infection of the filamentous coliphage of the Ff family are well characterized. The fd bacteriophage shares 98% identity with the genomes of phages M13 and f1. fd phage consists of a single-stranded DNA genome of about 6.4 Kb surrounded by a coat of thousands of copies of a small α-helical protein, pVIII. This major coat protein forms a filamentous capsid with a few copies of minor proteins at the filament ends. At one end of the phage capsid there are three to five copies of the surface exposed pIII and its accessory protein, pVI, the first proteins to interact with the *E. coli* host during infection. The phage coat's length can vary depending on the phage type, with the number of pVIII copies adjusting to accommodate the size of the single stranded genome it packages (Clackson and Lowman. 2004; Barbas et al., 2001; Kaya, et al 1998 Waldor et al. 2005).

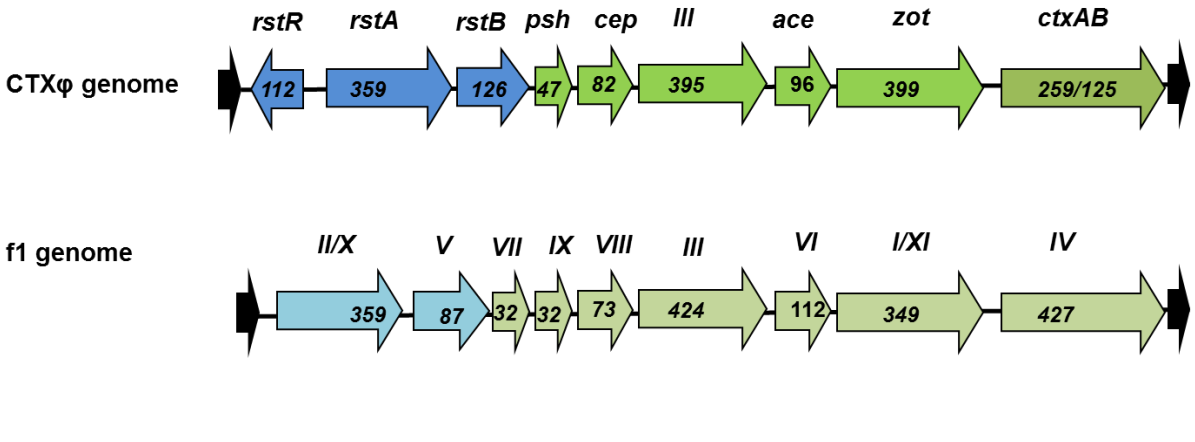

Figure 1-6. **CTXφ genome shares structure and gene organization homology with *E. coli* filamentous coliphage of the Ff family (M13, fd, f1) (Davis & Waldor, 2003).** Numbers are aminoacids per gene.

1.2.1.1. The Ff phage minor coat protein pIII

The Ff minor coat protein pIII is translated as a pre-protein with an 18-amino acid signal peptide that is removed by the bacterial Sec machinery, leaving a 406-amino acid mature protein (Beck and Zink, 1981). Mature pIII is organized into three distinct functional domains, N1, N2, and C, which are linked by glycine-rich segments of low structural complexity, LCR1 and LCR2 (Fig. 1-7) (Stengele et al., 1990) The first two pIII domains, pIII-N1 (residues 1 to 86) and N2 (residues 105 to 236), are required for Ff adsorption and entry (Stengele et al., 1990) Ff pIII-N1 and pIII-N2 bind to the *E. coli* coreceptors TolA and F pili, respectively (Deng et al., 1999; Riechmann and Holliger, 1997). The third domain C (residues 270 to 406), is required for the assembly and release of Ff phage particles from host cells (Crissman and Smith, 1984). The hydrophobic C-terminal segment is required for

insertion of the virion into the inner membrane during phage uptake, and for anchoring mature III into the inner membrane prior to incorporation at the tip of an assembling phage.

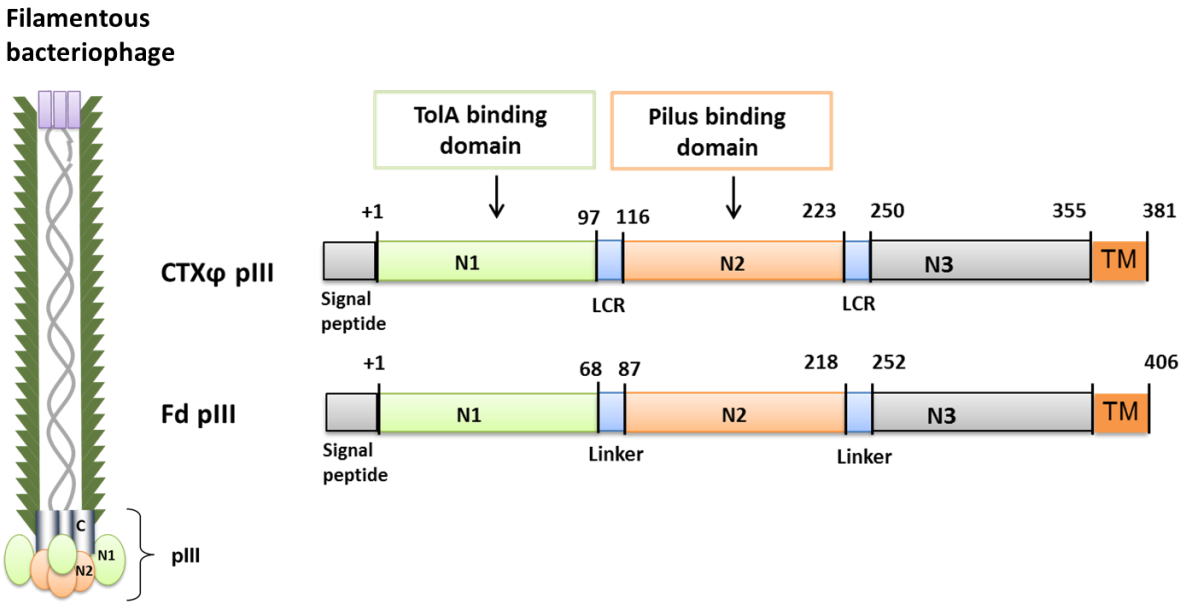

Figure 1-7. Diagram organization of pIII CTXφ and pIII fd. Based on its amino acid sequence the pIII protein is divided into 3 domains, an N-terminal domain (N1), a central domain (N2) and a C-terminal domain (N3). These domains are separated by glycine-rich flexible linkers and possess a highly hydrophobic terminal region that is predicted to be a transmembrane domain (TM) (Heilpern and Waldor, 2003). The fd phage pIII domains are predicted to be homologous to the CTXφ phage pIII domains. The N1 domain is the TolA binding domains in both phages (Ford et al., 2010; Deng et al., 1999; Riechmann and Holliger, 1997) and Fd pIII N2 domain has been shown to be the pilus binding domain. CTXφ pIII N2 is similarly predicted to be the pilus binding domain (Heilpern and Waldor, 2003).

1.2.1.2. Ff phage infection mechanism

The Ff phage binds to *E. coli* using pIII, 4-5 copies of which are located at the phage tip, in a dynamic two-step process to initiate infection. First, the central N2 domain of pIII binds to the F pilus, in a proposed tip to tip interaction (Deng et al., 1999; Riechmann and Holliger, 1997). Once this interaction occurs, pIII undergoes a conformational change that exposes the previously buried TolA binding site on pIII-N1 (Holliger et al., 1999; Lubkowski, et al., 1999). After pIII binding, F pilus is thought to spontaneously retract (Russel, 1998) bringing the phage tip across the *E. coli* outer membrane and into the periplasm, where the pIII-N1 domain contacts the C-terminal domain of the periplasmic protein, TolA (Fig. 1-8) (Riechmann and Holliger, 1997). The mechanisms by which the F pilus retracts and the bacteriophage gains entry into the periplasm to bind to TolA are not well understood.

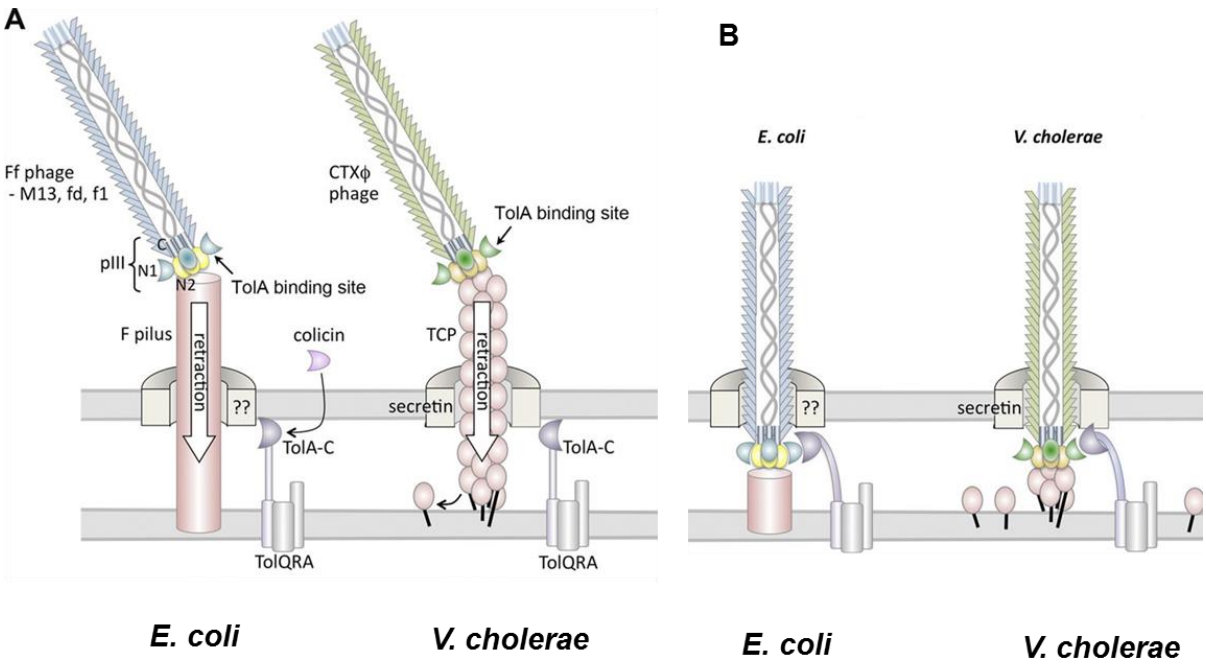

Figure 1-8. Comparison of model for uptake of filamentous phage by *E. coli* and *V. cholerae*. A) Phages bind to their respective pili via the N2 domain of pIII (Here pIII domains are referred as D or N interchangeably). In the case of the Ff phage, this interaction induces a conformational change that exposes the TolA binding site of N1. B) Pili retract, transporting the phage tip through the pilus secretin channel into the periplasm where the N1 domain of pIII interacts with the C-terminal domain of TolA. (Ford et al., 2012).

1.2.2. CTXφ phage genome and structure

Like the Ff family phage, CTXφ has a single stranded, circular DNA that is 7 Kb long. The organization of the CTXφ genome is similar to that of Ff, with a core region containing genes *cep, orfU, ace, zot, ctxA and ctxB,* which encode proteins pVIII, pIII, pVI, pI, CtxA and CtxB, respectively (Fig. 1-9). Flanking the core sequence are one or more repetitive sequence groups, which code for proteins responsible for expression of the phage genome and its integration into the *V. cholerae* chromosome, as described in Section 1.1.4.2. pVIII is homologous in sequence to the M13 pVIII and is predicted to be the major coat protein; it is a small α-helical protein that forms the long cylindrical phage coat packaging the DNA genome. Three to five copies each of the minor coat proteins pIII and pVI, are localized to one end, and single copies of pVII and pIX localized to the other end (Waldor and Mekalanos, 1996; Heilpern and Waldor, 2000).

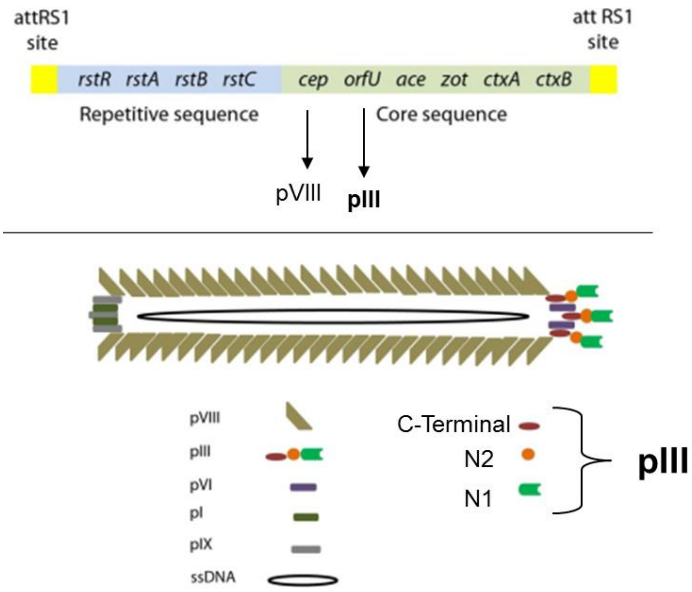

Figure 1-9. Structure of filamentous cholera phage CTXφ.

1.2.2.1. CTXφ minor coat protein, pIII

Though CTXφ pIII has no recognizable sequence homology to the Ff pIII proteins it has a similar domain organization to Fd phage pIII, with a 19-amino acid signal peptide and a mature protein composed of three domains: N1, N2 and a C-terminal domain (C), which are separated by serine and proline rich, low complexity regions (Fig. 1-7) (Heilpern and Waldor, 2003). The CTXφ pIII-C contains a very hydrophobic segment that likely represents an inner membrane anchor.

Heilpern and Waldor (2003) showed that pIII of CTXφ, like pIII of Ff phage, is responsible for host specificity (2003). They generated Fd phage hybrids where they fused domains N1, N2 or N1N2 of CTXφ pIII to full length fd pIII, which normally infects *E. coli*. They performed phage infection experiments where they showed that the hybrid Fd phage can infect *V. cholerae* in a TCP-dependent manner. Both pIII N1 and N2 of CTXφ are necessary for efficient infection *of V. cholerae* by fd phage. In contrast, D3 is not required for infection but it is necessary for virion assembly. Further, their studies indicated the CTXφ pIII-N1 is absolutely required for infection of *V. cholerae* since phage infectivity is completely abrogated in Fd phage-CTXϕ pIII fusions lacking CTXφ pIII-N1. Moreover, CTXφ pIII-N2 is needed for efficient infection but is not completely essential since phage lacking the N2 domain were still able to infect *V. cholera* cells, although at much lower levels.

Ford *et al.* (2012) demonstrated a direct interaction between the CTXφ pIII domain N1 and TolA and solved a crystal structure of this complex. They showed that despite low sequence identities between N1 of CTXφ and Ff phage M13,

these domains have similar topologies, in which a core β-barrel structure stabilized by disulfide bonds at similar locations. Surprisingly though, CTX and M13 pIII N1 domains bind to opposite faces of the C-terminus of TolA (Ford et al., 2012).

1.2.3. CTXφ phage infection mechanism

The mechanism of CTXφ infection of *V. cholerae* is thought to parallel that of the fd phage in *E. coli* (Fig. 1-8) due to similarity in structure, gene organization and function of pIII sub-domains (Deng and Perham, 2002). As shown by Heilpern and Waldor (2003), CTXφ phage infection of *V. cholerae* begins with CTXφ phage binding to TCP via the phage minor coat protein, pIII. TCP is the primary CTXφ receptor. CTXφ infection studies showed that *V. cholerae*, mutants that are unable to produce TCP, are infected by CTXφ phage at much lower levels than wild type *V. cholerae* (Heilpern and Waldor, 2003; Ford et al., 2012). It is predicted that CTXφ pIII-N2 is the pilus binding domain (Heilpern and Waldor, 2003) and that it binds to TcpA, the major subunit of TCP (Kirn et al., 2000), but nothing is known about the specificity of binding or how the phage is transported across the outer membrane where pIII-N1 contacts the C-terminal domain of TolA in the *V. cholerae* periplasm. TolA is anchored in the inner membrane via its N-terminus and it is part of the TolQRA complex which is required for outer membrane stability and uptake of bactericidal group A colicins (Ford et al., 2012; Karlsson et al., 2003). Following contact of pIII N1 with TolA, The CTXφ phage sheds its protein coat in the inner membrane and releases its DNA into the *V. cholerae* cytoplasm (Davis and Waldor, 2000). Within the cytoplasm, the bacterial DNA polymerase synthesizes a complementary (-) DNA strand from the CTXφ (+) single-stranded

genome to produce the double-stranded covalently closed circular replicative form, pCTX. Multiple copies of pCTX integrate site-specifically into *V. cholerae* chromosome 1 homologous region attRS1 as tandem prophage (Fig. 1-10) CTXφ does not encode its own integrase but recruits two host-encoded proteins, XerC and XerD, to accomplish integration (Huber and Waldor, 2002). Phage proteins are translated from mRNA transcribed from the pCTX fragment. CTXφ (+) ssDNA representing the phage genome can be produced from either CTXφ prophage or pCTX. This (+) ssDNA is packaged into CTXφ phage particles at the inner membrane and secreted from the cell via the Type 2 Secretion System (Fig. 1-10) (Davis et al., 2000; Davis and Waldor, 2000).

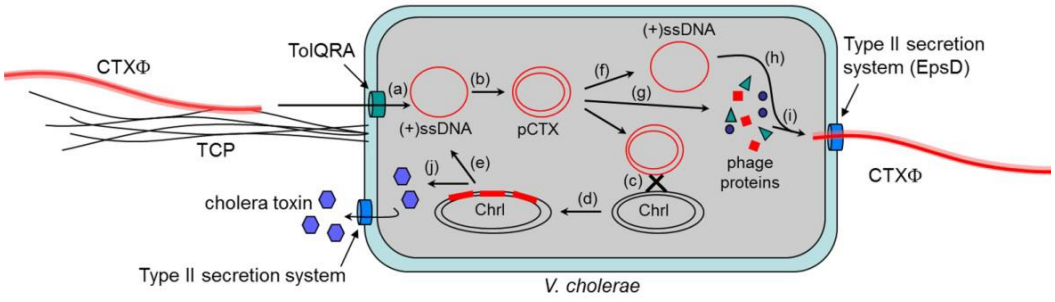

Figure 1-10. Model of CTXφ phage infection mechanism.

1.3. Type IV pili (T4P)

V. cholerae TCP, the primary receptors for CTXφ, belong to a large class of pili, the Type IV pili. These thin, long filaments are expressed on the surfaces of many Gram-negative bacteria, some Gram-positive species and archaea. They are polymers of hundreds or thousands of copies of the major pilin subunit. These robust filaments are 6-9 nm in diameter and several microns in length (see Fig. 1-1). They can resist tensile forces of up to 100–150 pN (Berry and Pelicic, 2015; Craig and Li, 2008; Maier et al., 2002; Melville and Craig, 2013). T4P assemble from pilin subunits in the bacterial inner membrane and grow across the periplasm and through a multimeric gated channel in the outer membrane called a secretin. Type IV pili are dynamic filaments that facilitate a broad array of functions. These functions, which vary depending on the species, include adhesion to host cells, twitching motility, microcolony formation, bacteriophage and DNA uptake, and secretion of colonization factors (Burrows, 2005; Craig et al., 2004). Due their central role in bacterial pathogenesis Type IV pili are of great interest and they are attractive targets for vaccines and therapeutics.

1.3.1. Type IV pilins

Type IV pili are assembled from thousands of the major pilin subunits. The major pilins are unique for each bacterial species but share some basic structural features: a homologous and hydrophobic N-terminal segment which is ~25 residues long with an invariant glutamate at position 5. The N-terminal ~53 residues form an extended α-helix, α1; the hydrophobic N-terminal half of this helix, α1-N, protrudes from the protein and the C-terminal half, α1-C, is embedded

in a globular domain (Fig. 1-11). α1-C interacts with an anti-parallel four- to five-stranded β-sheet with a conserved cysteine pair that forms a disulfide bond linking the C-terminal segment to the β-sheet (Horiuchi and Komano, 1998; Li et al., 2012; Strom and Lory, 1993; Pasloske and Paranchych, 1988).

The Type IV pilins are synthesized with an N-terminal signal peptide that is removed by a dedicated pre-pilin peptidase (Strom and Lory, 1993). The Type IV pilins are traditionally classified into two sub-groups: Type IVa (T4a) and Type IVb (T4b), on the basis of the lengths of their signal peptide and mature protein sequence. The T4a pilins are found in plant, animal, and human pathogens including *Pseudomonas aeruginosa*, *N. gonorrhoeae*, *N. meningitidis* and *Dichelobacter nodosus*, as well as in environmental genera such as *Thermus*, *Myxococcus*, and others. The T4b class is characteristic of enteric bacteria such as enteropathogenic, and enterotoxigenic *Escherichia coli, Salmonella enterica*, and *Vibrio cholerae.* Some species such as *P. aeruginosa* and *V. cholerae* can express multiple kinds of T4P (Bentzmann et al., 2006; Giltner, Rana et al., 2011).

Type IV pili of both classes share the same architecture. The N-terminal α-helices are arranged in a helical array forming the hydrophobic core of the pilus, with the C-terminal globular domains loosely packed on the filament surface (Fig. 1-11) (Craig et al., 2004; Kolappan et al., 2016; Li et al., 2012). The invariant glutamate at position 5, Glu5, of the pilin subunit is necessary for pilus assembly (Kirn et al., 2000; Li et al., 2012; Strom and Lory, 1993; Pasloske and Paranchych, 1988). Further, it has been proposed that an electrostatic attraction between Glu5 on the incoming pilin subunit and the positively-charged N-terminal amino group on the terminal subunit in the growing pilus (N1+) contributes to subunit docking

(Fig. 1-13) (Craig et al., 2006; Li et al., 2012). CryoEM structures of T4P from *N. meningitidis*, *N. gonorrhoeae* and *P. aeruginosa* support this arrangement (Kolappan et al., 2016).

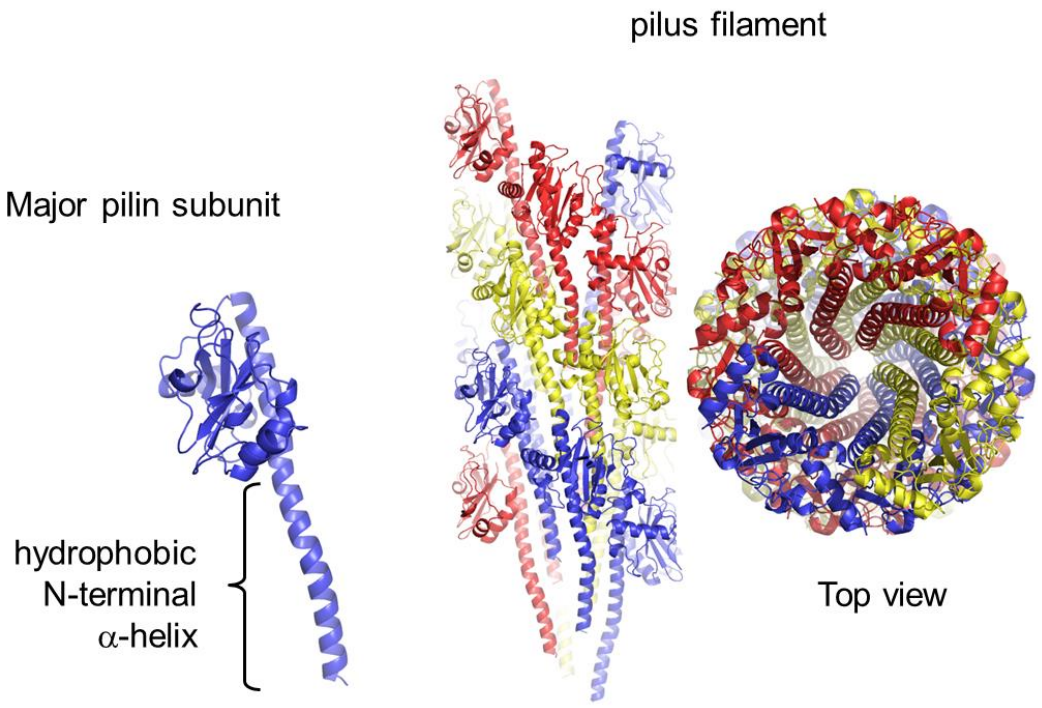

Figure 1-11. T4P major pilin subunit and filament structures. Pilus filaments are comprised of thousands of copies of the major pilin subunit. X-ray crystal structure of the *V. cholerae* major pilin subunit and pseudoatomic resolution structure of the pilus filament, determined by cryo-electron microscopy (Li et al., 2012).

1.3.2. Type IV pilus assembly and retraction

Polymerization of the major pilin subunits into surface-displayed pili is accomplished by an assembly machinery that spans the Gram-negative bacterial envelope. This machinery is comprised of as few as 9 proteins or as many as 40 components depending on the pilus and the bacterium (Taylor et al. 1987; Stone et al. 1996). Nevertheless, there are conserved components among all of these systems: the major pilin subunit, a secretin channel, an assembly ATPase, an inner membrane core protein and an alignment complex that forms a conduit for the pilus, connecting the inner membrane components with the secretin channel (Fig. 1-12) (Berry and Pelicic, 2015; Karuppiah et al., 2016; Leighton et al., 2015). Based on structural and biochemical analysis, we have proposed a working model for T4P assembly (Fig. 1-13) (Craig and Li, 2008; Kolappan et al., 2016; Ng et al., 2016).

Prior to pilus assembly pilin subunits are anchored in the inner membrane via their hydrophobic α1N. During pilus assembly, subunits dock into the base of a growing pilus at the inner membrane, attracted by an electrostatic interaction between the conserved negatively charged Glu5 residue on the incoming subunit and the positively charged amino nitrogen N-terminal residue of the preceding subunit (Figure 1-13). In the recent ~ 6 Å cryo-electron microscopy reconstruction of the *N. meningitidis* Type IV pilus, Kolappan *et al* (2016) showed a bridge of electron density connecting the N-terminal α-helices, consistent with a Glu5:N1+ salt bridge. Upon addition of each pilin subunit, the pilus is extruded a short distance, 8–10 Å, out of the membrane which is equivalent to the axial rise per subunit in the helical pilus. This motion opens up space for the next pilin subunit to

dock (Craig et al., 2006; Kolappan et al., 2016; Li et al., 2012). Pilus extrusion is driven by a hexameric assembly ATPase, located at the cytoplasmic face of the inner membrane (Yamagata et al., 1983) which undergoes a conformational change upon ATP hydrolysis. This change is thought to be transmitted through an inner membrane platform protein that performs the extrusion step (Anantha et al., 1998; Tripathi and Taylor, 2007). Pilus assembly is a continuous process until retraction is triggered.

In addition to the assembly ATPase, most T4P systems possess a retraction ATPase, which is required to depolymerize or retract the pili by an unknown mechanism (Anantha et al., 1998; Wall and Kaiser, 1999; Wolfgang et al., 1998). The T4a pilus systems, as well the T4b bundle forming pili (BFP) from enteropathogenic *E. coli*, include/possess a retraction ATPase (Fig. 1-12) (Brossay et al., 1994). Pilus retraction likely occurs by reversing pilus assembly, facilitating translocation of the pilin subunits from the base of the growing pilus back into the inner membrane. Retraction has been demonstrated for several T4a pili including *P*. *aeruginosa*, *N. gonorrhoeae*, *M*yxococcus *xanthus* and *Streptococcus sanguinis,* using biophysical methods such as total internal reflection fluorescence microscopy, optical tweezers and elastic micropillars assays (Biais et al., 2010; Biais et al., 2008; Clausen et al., 2009; Gurung et al., 2016; Maier et al., 2002; Merz et al., 2000; Skerker and Berg, 2001; Zaburdaev et al., 2014). T4P can retract with forces of 100–150 pN in a retraction ATPase-dependent manner (Maier et al., 2002). Recently retraction was also demonstrated for the *V. cholerae* Type IVb pilus, TCP, despite its lacking a retraction ATPase (Ng et al., 2016). Retraction allows key pathogenic functions such as twitching motility, microcolony formation,

exoprotein secretion and DNA and bacteriophage uptake into the cell (Maier and Wong, 2015; Merz et al., 2000; Zaburdaev et al., 2014).

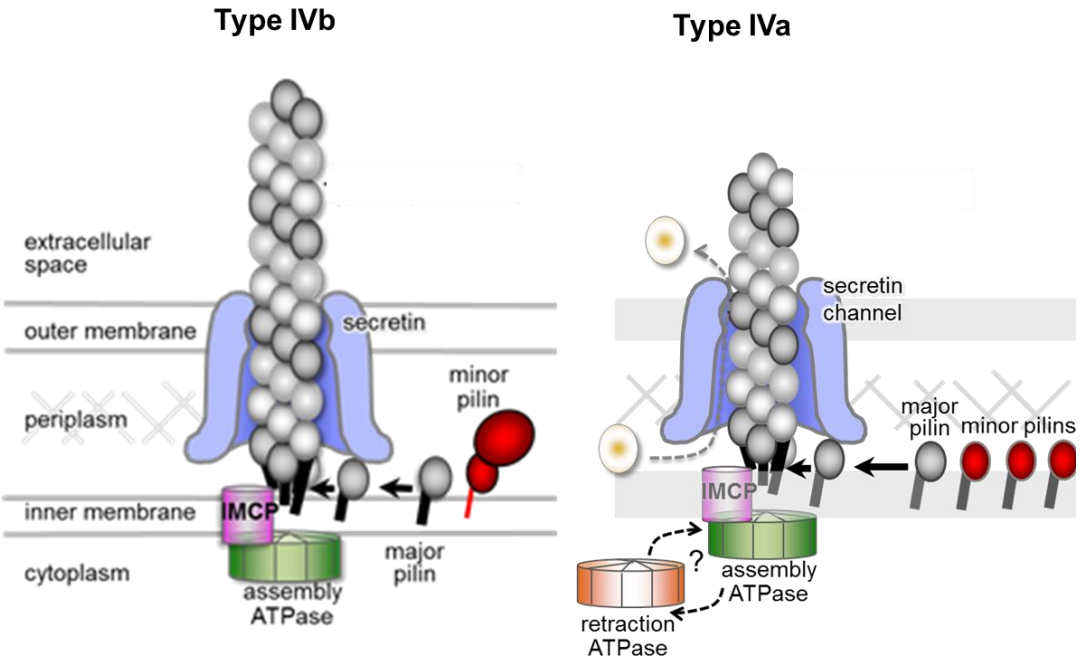

Figure 1-12. General comparison of the T4P assembly machinery among T4b and the more complex T4a system. Conserved components include the major pilin subunit (grey), a secretin channel (blue), an assembly ATPase (green), an inner membrane core protein (IMCP) shown in purple, and an alignment complex (not shown, formed by multiple proteins) that forms a conduit for the pilus and connects the inner membrane components with the secretin channel. T4b pili lack retraction ATPase and have a single large minor pilin. T4a pili have a retraction ATPase that powers pilus retraction and possess multiple minor pilins similar in size and structure to the major pilin.

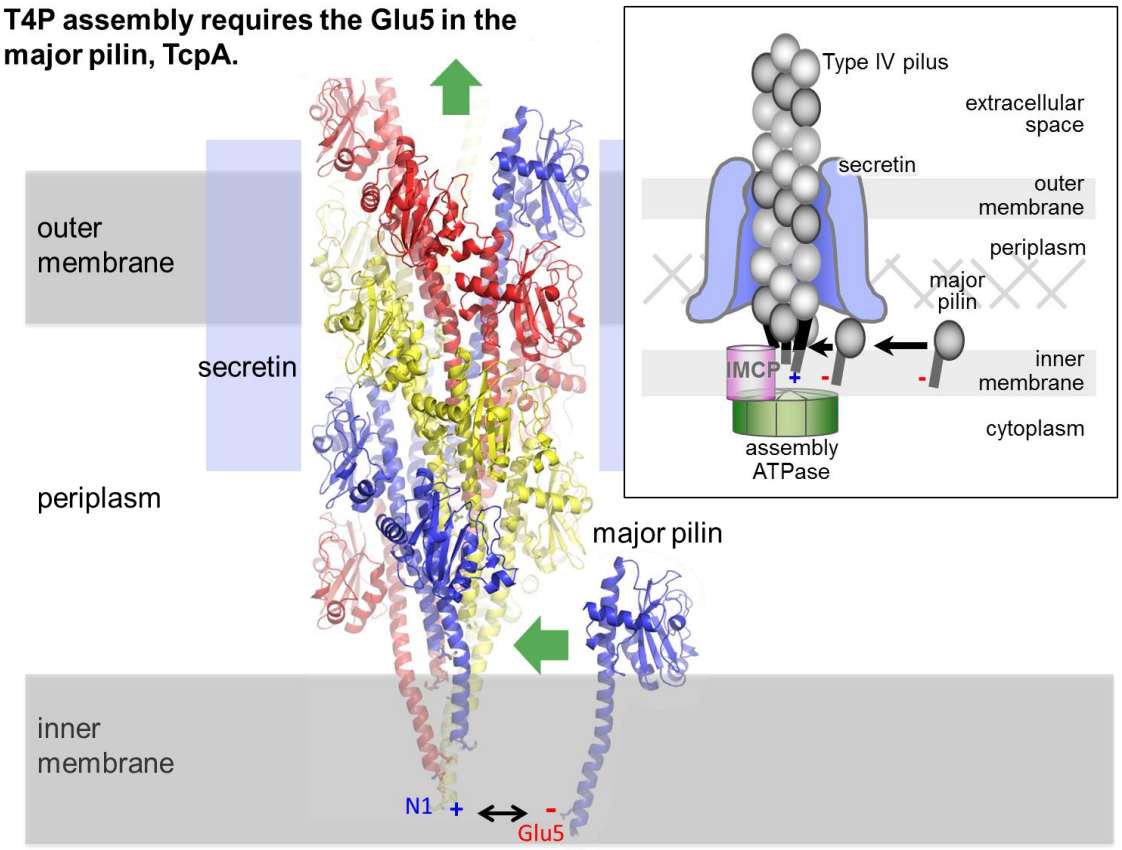

Figure 1-13. Model for T4P assembly. Major pilin subunits are thought to dock into the base of a growing pilus at the inner membrane, attracted by an interaction between the conserved negatively charged Glu5 residue on the incoming subunit and the positively charged amino nitrogen N-terminal residue (N1+) of the preceding subunit. The pilus is extruded a short distance, 8–10 Å, out of the membrane by a hexameric assembly ATPase which undergoes a conformational change upon ATP hydrolysis. This change is thought to be transmitted through an inner membrane platform protein (IMCP) that performs the extrusion step. This motion opens up space for the next pilin subunit to dock (Craig et al. 2006; Kolappan et al., 2016; Li et al., 2012).

1.3.3. T4P are related to the Type II secretion system

The core T4P assembly machinery is structurally and functionally related to the bacterial type II secretion (T2S) system (Fig.1-14). Many Gram-negative bacteria use the T2S system to translocate folded proteins from the periplasm across the outer membrane and into extracellular space. *V. cholerae* secretes cholera toxin via this system (Sandkvist et al., 1997). The T2S system is thought to assemble pseudopili which are short periplasmic filaments formed by pilin proteins that grow through the periplasm, but do not grow past the outer membrane (Korotkov and Hol, 2013; Korotkov et al., 2012; M Sandkvist, 2001). T2S pseudopili are comprised of multiple copies of the major pseudopilin subunit, which shares amino-terminal sequence homology to the T4 pilin proteins, including the invariant glutamate at position 5, and is similar in structure to the Type IV pilins. Additionally, overexpression of pseudopilins results in the formation of surface displayed pseudopili, consistent with their evolutionary relationship with T4P (Sauvonnet et al., 2000). T4P systems can also secrete effectors (Megli et al., 2013; Kirn et al., 2003). Despite lacking a retraction ATPase, the T2S system pseudopili are thought to undergo cycles of rapid assembly and disassembly to facilitate function and secretion of substrates in a piston-like mechanism (Korotkov et al., 2012).

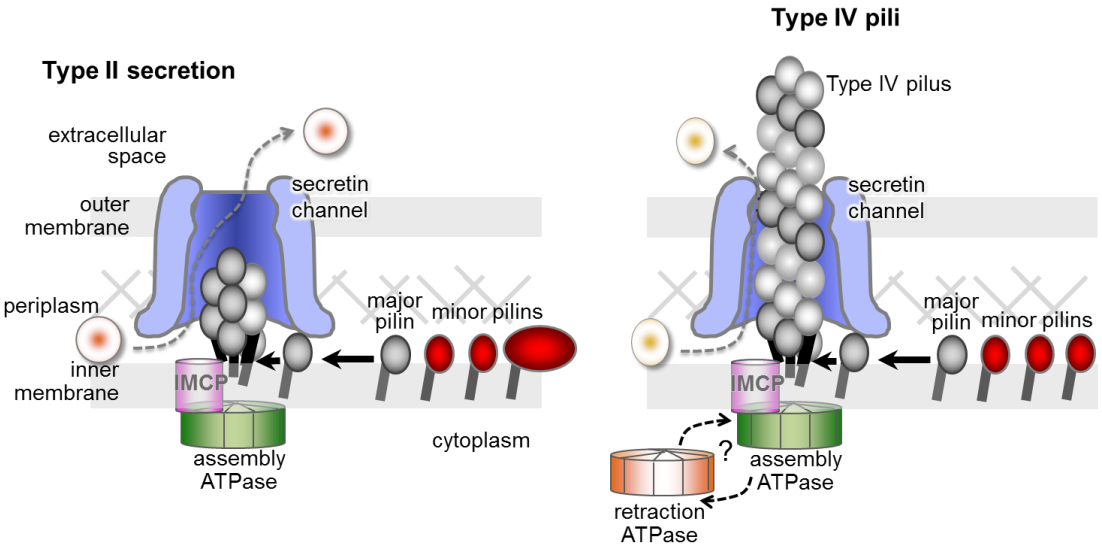

Figure 1-14. The Type IV pilus system is closely related to the bacterial Type II secretion system. The T2S system assembles pseudopili which are short periplasmic filaments formed by pilin proteins that grow through the periplasm but unlike T4P they do not grow past the outer membrane. T2S, like T4b, lack a retraction ATPase and can have minor pilins that are much larger than the major pilin.

1.3.4 Minor pilins

In addition to the major pilin, which is the structural unit for the T4P and T2S pseudopili, these systems typically also possess several minor pilins, pilin-like proteins that share N-terminal homology with the major pilins but are expressed at much lower levels than the major pilins (Fig. 1-14). Minor pilins are involved in T4P and T2S dynamics and functions but their mechanisms are not well understood. The minor pilins are required for both pilus assembly and secretion in *P*. *aeruginosa*, *N*. *gonorrhoeae*, EPEC and *V. cholerae* (Cisneros et al., 2012a; Cisneros et al., 2012b). The minor pilins are thought to form a priming complex to facilitate pilus assembly. In *P. aeruginosa* the T4P minor pilins, FimU, PilV, PilW, PilX and PilE are thought to form a complex that associates with the adhesion protein PilY1. They have been shown to incorporate into surface displayed pili at low levels (Nguyen et al., 2015). In the ETEC T2S system the minor pseudopilins, GspI, GspJ, and GspK were crystallized in complex (Korotkov and Hol, 2008). GspK is the largest of the minor pilins, resembling the major pilins but with an additional bulky α-helical protrusion in its C-terminal domain. It has been hypothesized that GspK is the first subunit in assembly and acts as a large cap that prevents the pseudopilus from passing through the outer membrane secretin channel (Korotkov and Hol, 2008, 2013; Korotkov et al., 2012). Thus, the pseudopilus would grow through the periplasm and stalls at the secretin channel, simultaneously extruding substrate that has homed to the vestibule of the channel (Fig. 1-14) (Reichow et al., 2010). While most minor pilins have the invariant N-terminal Glu5 found in the major pilins, GspK has a hydrophobic amino acid at this

position. As the first subunit in the pilus, Ng et al. (2016) proposed that GspK does not require Glu5 as it would not need to neutralize the N1+ charge of an existing pilin subunit in the filament, but it would need its positively charged N-terminal residue to neutralize Glu5 of the incoming pilin. Despite the important role minor pilins play in pilus assembly their mechanisms for priming pilus assembly are poorly understood, and there is no direct evidence showing a minor pilin at the tip of a T4P or T2S pseudopilus.

Some T4P systems also possess one or more non-core minor pilins that are not essential for pilus assembly but are required for pilus functions. For example, The *N. meningitidis* minor pilin PilX is not required for pilus assembly but has been shown to modulate signaling to host cells (Bernard et al., 2014; Brissac et al., 2012) and bacterial aggregation (Helaine et al., 2007; Imhaus and Duménil, 2014). Additionally, minor pilins have been proposed to function as regulators of pilus dynamics rather than mere initiators of filament assembly (Winther-Larsen et al., 2005). The minor pilins of T4P localize to the pilus fraction, based on immunoblots, and have been shown by immunogold labeling and transmission electron microscopy to be incorporated at low levels throughout the pilus (Giltner et al., 2010), although the quality of the gold labeling on these images is poor. Structural studies on minor pilins from several bacterial species reveal the conserved pilin fold consistent with their ability to incorporate into the pilus filament (Helaine et al., 2007; Nguyen et al., 2015a; Nguyen et al., 2015b). Additionally, in the *P. aeruginosa* T2S system, long pseudopilus filaments are formed when the GspK homolog, XcpX, is deleted and the major pseudopilin is overexpressed (Durand et al., 2005), suggesting that the minor pilin is needed for pseudopilin disassembly.

Importantly, the more simplistic T4b systems of ETEC and *V. cholerae* contain only a single minor pilin, which is implicated in both pilus assembly and retraction (Kolappan et al., 2015; Ng et al., 2016).

1.3.5 Type IVb pili of *V. cholerae* and ETEC

The Type IVb pilus systems are much simpler systems than the Type IVa systems (Fig. 1-12). Fewer than a dozen proteins encoded in a single operon are sufficient for Type IVb pilus assembly and functions (Fig. 1-15). The Type IVb systems in *V. cholera*e and enterotoxigenic *E. coli* (ETEC) bacteria lack a retraction ATPase and encode a single minor pilin instead of several. The minor pilin is significantly larger than the major pilin counterpart, similar to the GspK family of proteins in the T2S system. Because of their relatively simplicity and possession of a single minor pilin, these systems are ideal to study the role of the minor pilin in T4P functions.

ETEC is a rod-shaped Gram-negative bacterium with a molecular mechanism of pathogenesis similar to that of *V. cholerae*. Upon adhesion to the host intestinal epithelium, ETEC produces and secretes one or both of two enterotoxins, heat-labile toxin (LT), an ADP ribosylating AB5 toxin that is highly similar to cholera toxin, and heat-stable toxin (ST), a guanylate cyclase. ETEC possess one of two type IVb pili, CFA/III (Colonization Factor Antigen III) and Longus. These filaments mediate attachment to epithelial cells (Mazariego-Espinosa et al., 2010) adhesion to epithelial cells (Taniguchi et al. 2001). CFA/III and longus pili mediate bacterial self-aggregation, antimicrobial resistance, secretion of colonization factor, CofJ, and adherence to intestinal epithelial cells (Mazariego-Espinosa et al., 2010; Yuen et al., 2013). The gene clusters that encode the CFA/IIII and Longus proteins are

found on large virulence plasmids that also encode the ETEC toxins (Giron et al. 1997; Taniguchi et al. 2001; Girón et al., 1994).

The TCP of *V. cholerae* is a T4b pilus that is critical for colonization of the human small intestinal epithelium. TCP self-aggregate to hold *V. cholerae* in microcolonies that facilitate colonization of the host. TCP, like ETEC CFA/III, acts as a secretion system, transporting a colonization factor TcpF across the outer membrane. TCP are also the primary receptor for CTXφ (Lim et al. 2010; Taylor et al. 1987; Waldor and Mekalanos 1996;Kirn et al., 2003; Kirn et al., 2000; Megli and Taylor, 2013). All of these processes not only require pilus assembly but also pilus retraction (Ng et al., 2016). TCP-mediated aggregation is facilitated by pilus:pilus interactions (Lim et al. 2010; Kirn et al., 2000) and pilus retraction draws bacterial cells close together in microcolonies. TcpF secretion is thought to be enabled via rapid assembly and disassembly of TCP in a piston-like mechanism (Ng et al., 2016) similar to one that has been proposed for the T2S system (Korotkov et al., 2012). And CTXϕ infection cycle requires the bacteriophage to bind to TCP and to be taken into the periplasm, where pIII interact with TolA (Ford et al., 2012; Heilpern et al., 2003) initiating uncoating of the phage. Phage uptake likely requires the pilus to retract and bring the bacteriophage into the periplasm. Despite lacking a retraction ATPase, TCP were shown to be retractile by micropillar assays. Ng et al showed that a non-motile but piliated *V*. *cholerae* strain, Δ*flaA*, induces micropillars movements, whereas the non-piliated Δ*tcpB*/Δ*flaA* strain does not, indicating that micropillar movements are pilus-mediated.

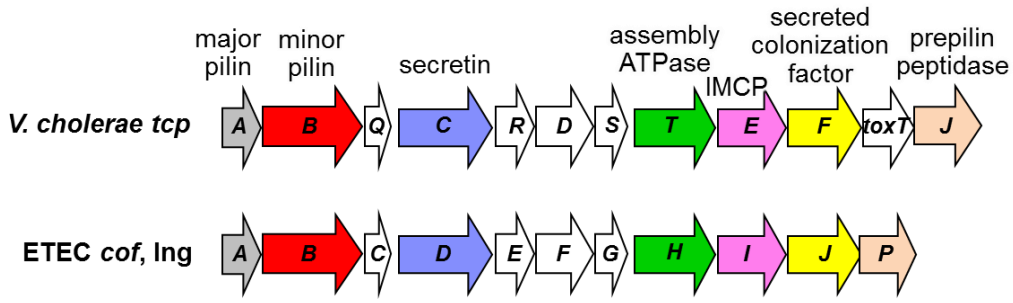

Figure 1-15. T4b pilus operon alignment of tcp and cof,lng. All three operons encode a single minor pilin (tcpB, cofB, lngB) and they each lack a retraction ATPase.

1.3.5.1. Minor pilins of ETEC and *V. cholerae*

CofB and TcpB are the minor pilins of ETEC and *V. cholerae* respectively. These minor pilins share gene synteny, and size, both being much larger than their major pilins. The N-terminal domain of the minor pilins shares amino acid sequence similarity with the N-terminal 25-residue polymerization domain (α1N) of their respective major pilins, including the conserved Glu5, but differ by having a much larger C-terminal region, similar to the GspK minor pilin of the T2SS. Kolappan et al. (2016) solved the 2 Å crystal structure of CofB. As predicted, CofB has a pilin domain very similar in fold to that of the ETEC major pilin CofA, (Fig. 1-16). Additionally, CofB possesses a unique extended C-terminal region with two small β-sheets (β-repeat sub-domains) and a C-terminal β-sandwich domain, all connected to the pilin domain by flexible linkers. The structure of TcpB has not yet been solved. Nonetheless, the alignment of the conserved N-terminal α1s and 6 cysteines of TcpB with CofB reveals shared residues and suggests a similar structure, except that TcpB has only a single β-repeat sub-domain, which is predicted to fold into the C-terminal β-sandwich domain (Fig. 1-17).

CofB and TcpB have similar functions in Type IVb pilus dynamics. Our group hypothesized that due their large size, these minor pilins might incorporate into a growing pilus and stall pilus assembly, perhaps by preventing passage of the pilus through the secretin channel, thus triggering retraction. Interestingly, TcpB was found to not only induce pilus retraction but assembly as well (Kolappan et al.,2015; Ng et al., 2016).

The ETEC minor pilin CofB from the CFA/III system is required for pilus assembly (Kolappan et al., 2015). CofB was the first minor pilin shown to initiate pilus assembly on its own. Given its role in initiating CFA/III pilus assembly, its structure and similarities with the minor pilin GspK, it was proposed that the CofB localizes at the tip of CFA/III as the first pilin subunit in the filament, and recruits the first major pilin to assemble the filament (Fig. 1-18). The flexible nature of the C-terminal domain would allow it to pack on the pilus tip and pass through the outer membrane secretin channel. Importantly, as the first priming pilin subunit, the positively charged N-terminal amine, N1+, of CofB would form an electrostatic interaction with Glu5 of the first incoming major pilin subunit, as seen in Figure 1-19, but the CofB Glu5 itself would not be necessary for pilus assembly.

Ng et al (2016) showed that TcpB is a key regulator of TCP dynamics with dual antagonistic roles in pilus biogenesis. They showed that TcpB is required for efficient TCP pilus assembly and functions. They obtained TEM images that show abundant TCP bundles for *V*. *cholerae* WT strain and few or no pili are observed in the Δ*tcpB* mutant which were subsequently restored in a tcpB-complemented strain. Not surprisingly, TcpF secretion and bacterial autoagglutination were found to be abrogated in the Δ*tcpB* mutant since TcpB is needed for pilus assembly. TcpB is present in the purified pilus fraction in minute quantities. The stoichiometry of the minor pilin, TcpB, to the major pilin, TcpA, in purified TCP was quantified using densitometry and anti-TcpA and anti-TcpB antibodies. The intensities of the immunoblot bands of each protein were compared with those of known concentrations of purified recombinant N-terminally truncated (ΔN-) TcpA and TcpB of known concentrations. It was found that purified TCP contain ~ 7000

molecules of TcpA for every TcpB subunit, or approximately 1 TcpB molecule per pilus, which was proposed to locate at the pilus tip (Ng et al., 2016).

Importantly, TcpB was shown to have an additional role as an initiator of TCP retraction. Based on the pilus assembly model of CofB (Fig. 1-18), Ng et al predicted that a TcpB Glu5 mutant would be able to initiate pilus assembly, as it still possesses its positively charged N1+, but would not be able to incorporate into the growing pilus to initiate pilus retraction, as it would need Glu5 to form a salt bridge with N1+ of the last subunit in the growing pilus, (Fig. 1-19). They showed that *V. cholerae* TcpB Glu5 mutants made greater than wild type levels of pili but their functions in autoagglutination and secretion of TcpF were impaired at levels consistent with the nature of the mutation. The most conserved change, to the negatively charged aspartate (E5D) showed a slight reduction in pilus functions; the Glu5Gln (E5Q) substitution, which results in loss of the negative charge but retains polarity showed higher degree of pilus functions impairment, and the Glu5Val, the most divergent substitution, to a hydrophobic side chain, resulted in a dramatic reduction functions. These results are consistent with TcpB-Glu5Val mutant initiating pilus assembly but not pilus retraction. Importantly, this mutant was unable to induce micropillars movements despite being fully piliated, and hence is non-retractile. Thus, TcpB initiates both pilus assembly and retraction in *V. cholerae* and is essential for pilus functions (Ng et al. 2016).

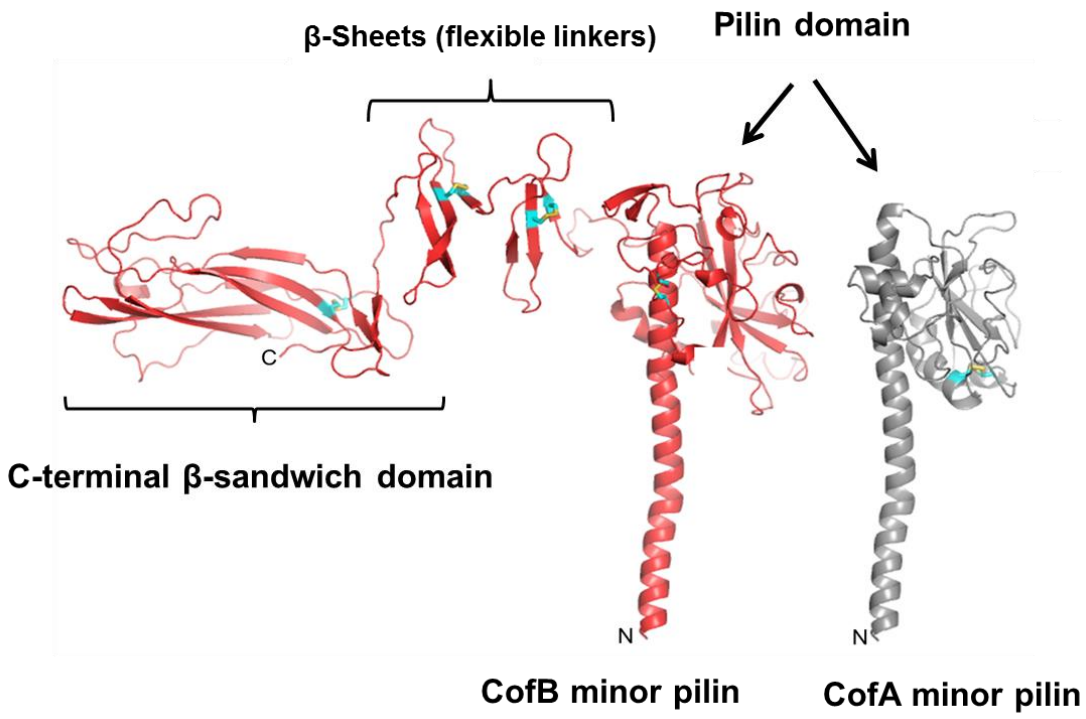

Figure 1-16. Comparison of the CofB minor pilin and CofA major pilins.

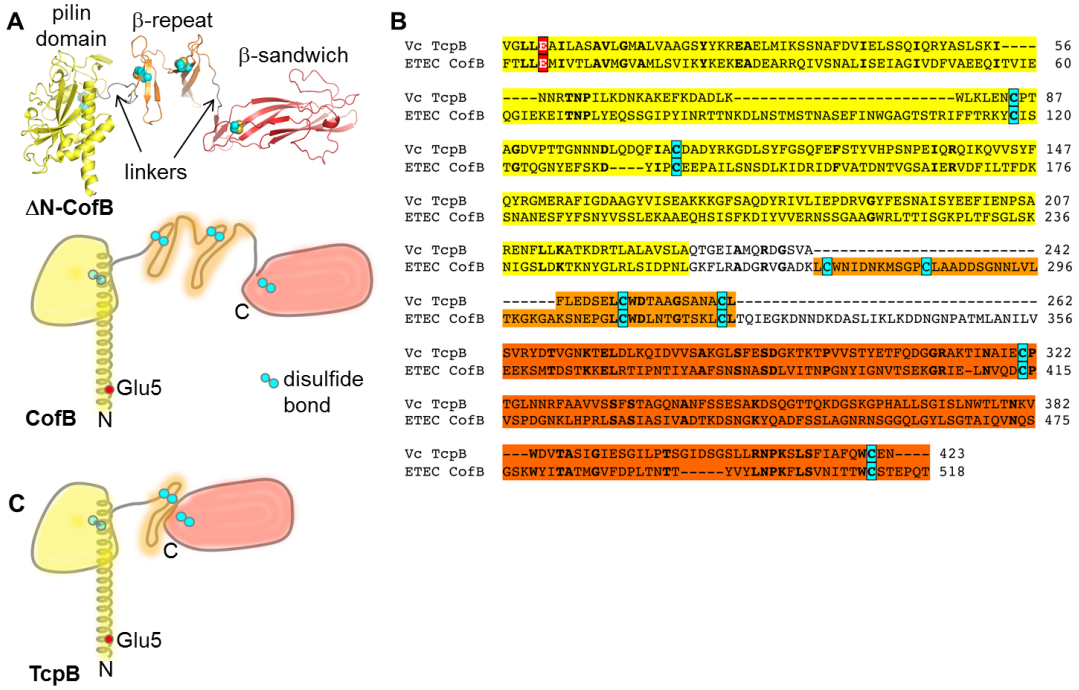

Figure 1-17. Comparison of the structure of CofB with the TcpB sequence. Alignment of the conserved N-terminal α1s and 6 cysteines of TcpB with CofB reveals shared residues and suggests a similar structure, except that TcpB has only a single β-repeat sub-domain, instead of two, that is predicted to fold into the C-terminal β-sandwich domain (Ng et al., 2016).

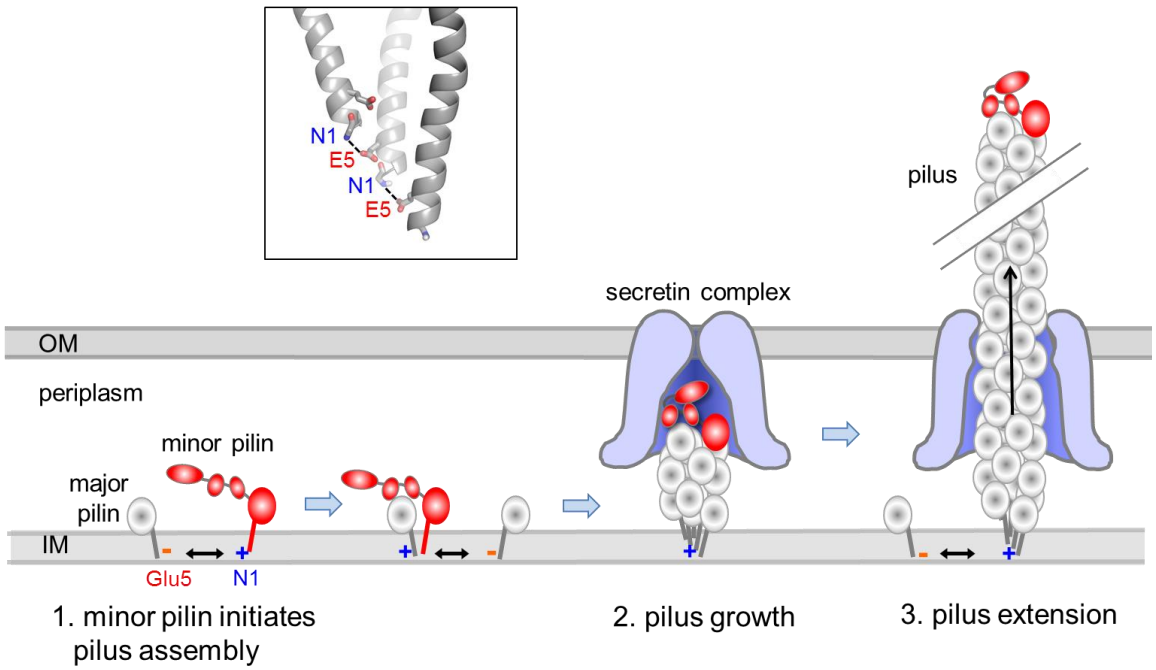

Figure 1-18. Model for CofB minor pilin-induced pilus assembly. Glu5 on CofB is not required for pilus assembly, as the first priming pilin subunit, the positively charged N-terminal amine, N1+, of CofB would form an electrostatic interaction with Glu5 of the first incoming major pilin subunit (Kolappan et al. 2015).

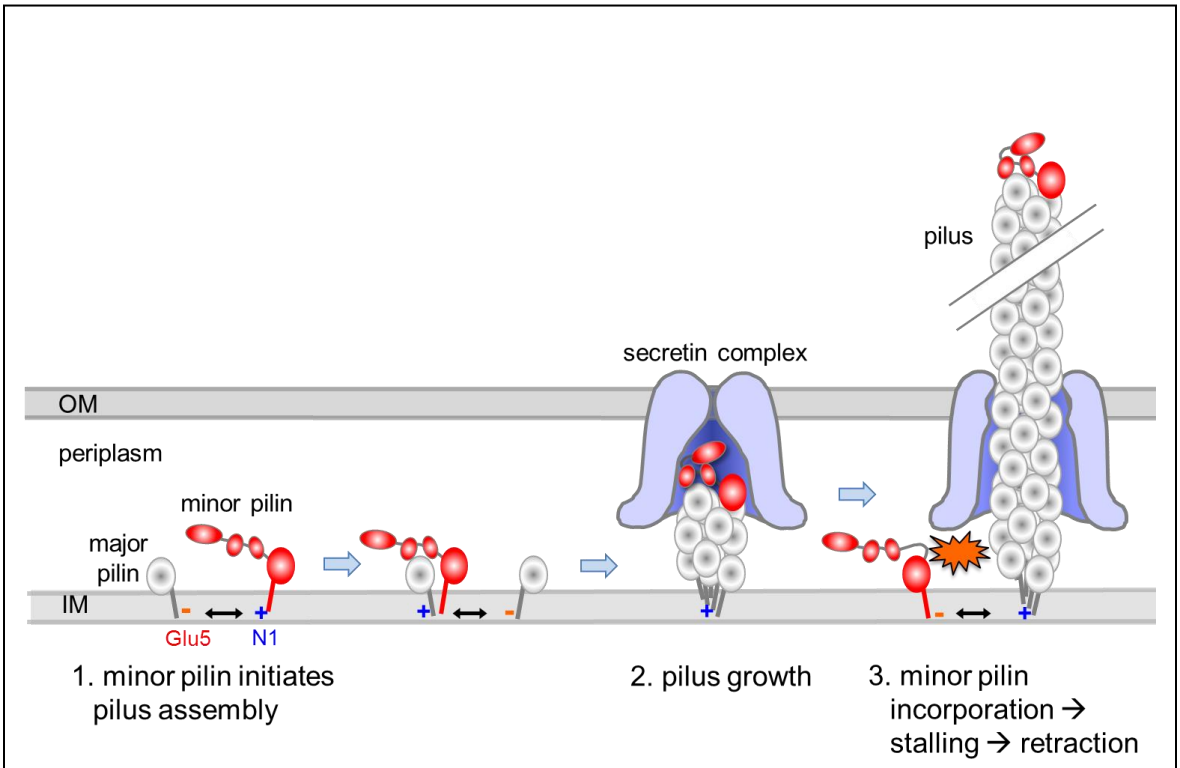

Figure 1-19. Model for CofB minor pilin-induced pilus retraction. Glu5 on CofB is not required for pilus assembly but it is required for pilus retraction. As Glu5 of CofB forms a salt bridge with N1+ of the last subunit in the growing pilus, that facilitates incorporation into a growing pilus and stalls pilus assembly, perhaps by preventing passage of the pilus through the secretin channel, thus triggering retraction (Ng et al., 2016).

1.3.5.2. The *V. cholerae* secretin complex

The secretin complex in the *V. cholerae* T4P system, is a gated outer membrane protein that facilitates the transport of proteins and macromolecular complexes from the periplasm across the outer membrane. Further, the secretin forms the channel that allows pilus growth across the outer membrane for display on the surface of bacterial cells (Bose and Taylor, 2005; Chang et al., 2017). Although the structure of *V. cholerae* secretin has not been solved, it is identified as a secretin protein since its C-terminus shares sequence similarity with other secretins. Secretins of other T4P systems and the *V. cholera*e T2S have been well characterized in terms of structure and function via cryoelectron microscopy and crystallization studies (Korotkov et al., 2011; Chami et al, 2005; Collins et al, 2004; Reichow et al., 2010; Yan et al., 2017). Secretins form gated outer membrane channels composed of 12-14 subunits with a diameter of approximately 50-80 Å to allow for secretion of proteins, pilus passage and DNA uptake (Chami et al., 2005; Collins et al., 2004; Korotkov et al., 2011). Recently, Chang et al (2017) used electron cryoelectron tomography methods to obtain a low resolution in situ averaged structure of the intact TCP assembly machinery with a TCP pilus present. The resulting averages and reconstructions of the TCP assembly machinery show that the secretin open gated diameter is ~8 nm, just large enough for the ~8 nm diameter TCP pilus to pass through it (Fig. 1-20). Additionally, and central to my project, the secretin is the channel through which the filamentous CTXφ phage is thought to cross the outer membrane into the periplasmic space

using TCP as its receptor. CTXφ is very similar in diameter size to the TCP pilus as seen in multiple transmission electron microscopy images (Ford et al. 2012).

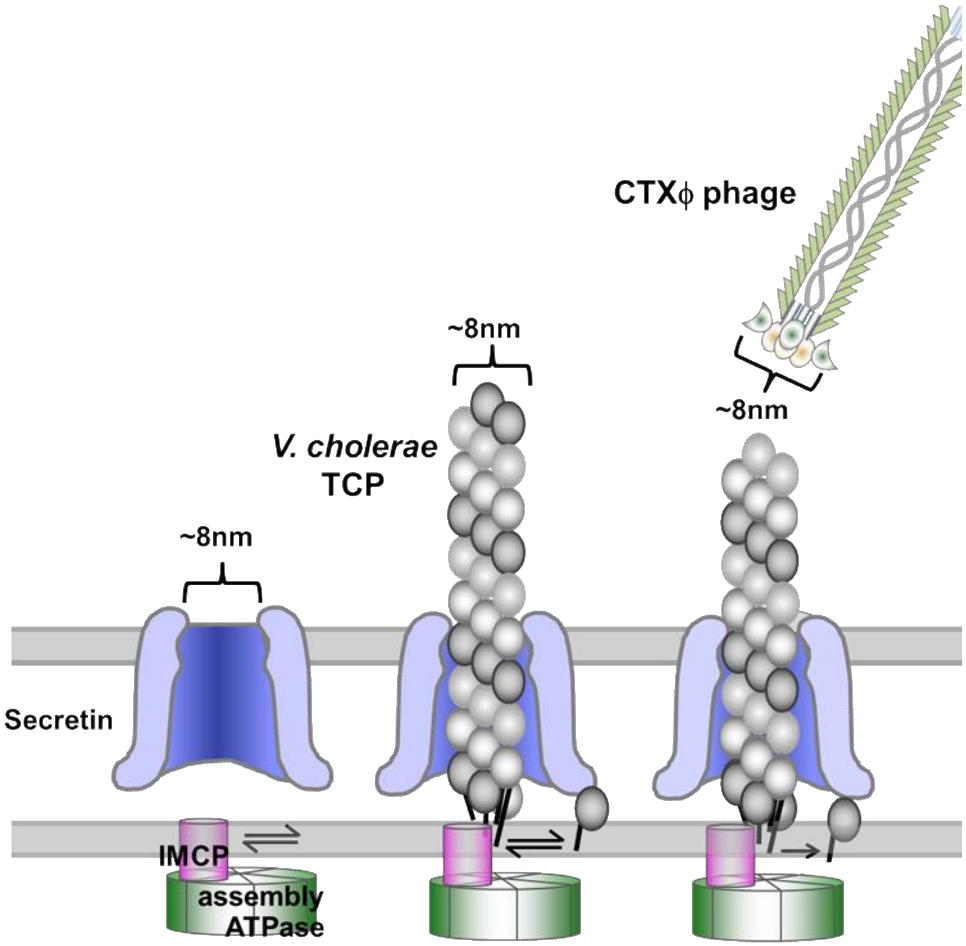

Figure 1-20. **Comparison of diameter sizes among Secretin, TCP and CTXφ phage in *V. cholerae*.** The secretin is barely wide enough to accommodate the TCP pilus. The secretin is the channel through which CTXφ phage is thought to cross the outer membrane via its TCP receptor. Inner membrane core protein (IMCP) in purple. Hexameric assembly ATPase in green.

1.4 Thesis Objective

Given what is known about the role of TcpB in TCP functions and the mechanism for CTXφ phage uptake in *V. cholerae*, we hypothesize that the CTXφ phage tip protein, pIII, binds to TcpB, located at the tip of TCP pilus. Following this pIII:TcpB interaction, CTXφ phage is then transported across the outer membrane via TCP retraction as if it were an extension of the pilus (Fig. 1-21).

The specific aims of this thesis project are:

1. Investigate the proposed CTXφ pIII:TcpB interaction.

2. Investigate the localization of TcpB within TCP.

3. Examine the role of TCP retraction in CTXφ phage uptake.

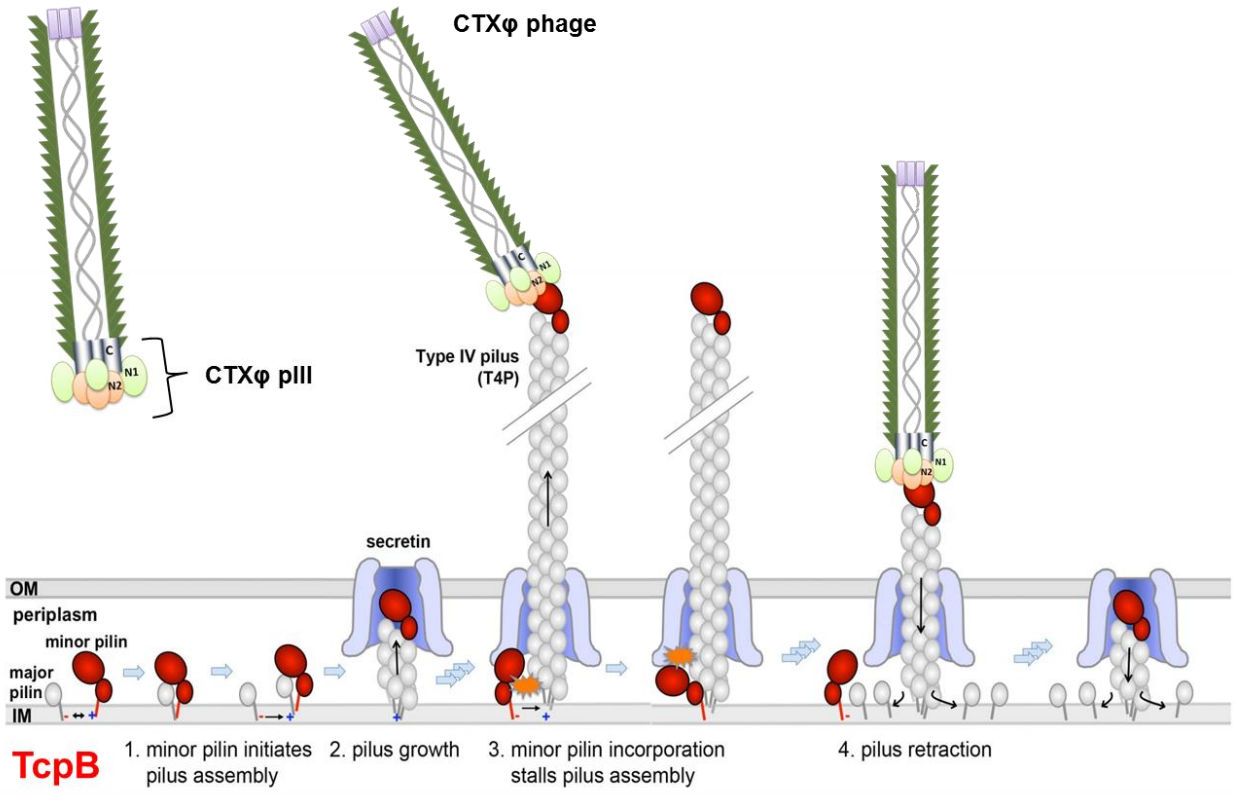

Figure 1-21. **Model proposed for CTXφ uptake by *V. cholera*.** The minor pili TcpB is shown in Red. Major pilin, TcpA, is shown in grey. It still remains unclear whether the minor pilin incorporates and is extruded along an assembling filament to induce retraction, or simply incorporates at the base of a growing filament to induce retraction without extrusion.

Chapter 2. Material and Methods

2.1. Bacterial Strains

Bacterial strains, plasmids, and primers are listed in Table 2.1. *E. coli* strains were grown in Lysogeny broth (LB) at 37 °C with appropriate antibiotics. *V. cholerae* strains, which are naturally resistant to streptomycin, were grown in LB, pH 6.5, streptomycin (Sm) at 30 °C on a Ferris wheel rotator to induce production of TCP. Antibiotics were used at a final concentration of 200 μg/ml streptomycin (Sm), 50 μg/ml kanamycin (Km), 100 μg/ml ampicillin (Amp). Antibodies used in ELISAs, phage transduction and immunogold labeling are listed in Table 2.2

Table 2.1. List of bacterial strains, strains and plasmids

Strain	Description	Source
***V. cholerae* O395**	Wild-type classical strain	Ron Taylor
V. cholerae CL101	Classical strain containing pCTX plasmid, produces CTXφ bacteriophage.	Ron Taylor
V. cholerae* SJK70 *ΔtcpA	O395 Δ*tcpA*	Kirn et al. (2000)
V. cholerae* YG003 *ΔtcpB	O395 Δ*tcpB*	Kirn et al. (2000)
***E. coli* (DH5α)**	*F− endA1 glnV44 thi-1 recA1 relA1 gyrA96 deoR nupG Φ80dlacZΔM15 Δ(lacZYA-argF)U169, hsdR17(rK− mK+), λ–*	Life Technologies
E. coli SHuffle T7	*F´ lac, pro, laclq / Δ(ara-leu)7697 araD139 fhuA2 lacZ::T7 gene1 Δ(phoA)PvuII phoR ahpC* galE (or U) galK λatt::pNEB3-r1-cDsbC (SpecR, laclq) ΔtrxB rpsL150(StrR) Δgor Δ(malF)3*	Life Technologies

Plasmid	Description	Source
pJMA10.1	A rhamnose inducible plasmid; Ap^R . pBAD22 derivative; araC replaced with PrhaB. Bla.	Ng et al, 2017
pJMA10.1-*tcpB*	containing the tcpB gene	Ng et al, 2017
pJMA10.1-*tcpBE5Q*	ptcpB with Gln5	Ng et al, 2017
pJMA10.1-*tcpBE5D*	ptcpB with Asp5	Ng et al, 2017
pJMA10.1-*tcpBE5V*	ptcpB with Val5	Ng et al, 2017
pET:15b	The pET-15b vector (Cat. No. 69661-3) carries an N-terminal His•Tag® sequence followed by a thrombin site and three cloning sites	Novagen
pET:24a(+)	Carries an N-terminal T7•Tag® sequence plus an optional C-terminal His•Tag® sequence.	Paetzel lab.
pMAL c2x	*E. coli* plasmid cloning vector designed for recombinant protein expression and purification using the pMAL Protein Fusion and Purification System (NEB #E8000S). The multiple cloning site (MCS) is positioned to allow translational fusion of the *E. coli* maltose binding protein (MBP, encoded by the *malE* gene) to the N-terminus of the cloned target protein.	New England Biolabs

Primer	Nucleotide Sequence	Source	Tube label Located in oligos MG box (-20ºC)
CTXφ pIII N1N2N3(1-355)-F-BamH1	5’ –GGAATTCAATATGTCCGCCAT CAA TTG TG– 3’	This work	B71
CTXφ pIII N1N2N3(1-355)-R-NdeI	5’ –CGTAGGATCCTTAGTGCAGGTT TTCA GAA AAG AGG GAG– 3’	Ford G.C. et al. 2012	pIII-R(1-360)_ B67
CTXφ pIII N1N2(1-232)-R-NdeI	5’ –CGTAGGATCCTTAAACGACAG TCCCACCGAGTC– 3’	Ford G.C. et al. 2012	pIII-R(1-238)_ B64
CTXφ pIII N2(117-232)-F-BamH1	5’ – GGAATTCCATATGAGTGCGTTCCCTT – 3’	This work	pIII N2 (117-232) FP_B75
CTXφ pIII N2(133-232)-F-BamH1	5’ – GGAATTCCATATGACTCTCAATCATG T CA– 3’	This work	B72
CTXφ pIII N2(133-218)-R-NdeI	5’ – CGTAGGATCCTTACCGAAGGACAT TAAG– 3’	This work	pIII (133-218) RP_ B73
pET22 pIII N1N2_R (1-232) XhoI	5’- CCGCTCGAGTTAAACGACAGTCCCA CC GAGTGAGTC-3’	This work	
pMAL pIII N1N2N3 (1-355)- F-BamHI	5'- CGCGGATCCTCCGCCATCAATTGTG AT CCTAATAC -3'	This work	
pMAL pIII N1N2N3 (1-355)- R-XbaI	5’- GCTCTAGATTAATGATGATGATGATG A TGGTGCAGGTTTTCAGAAAAGAGGG AG-3’	This work	
pET-24a-d(+) pIII N1N2N3 (1-355) F-BamH I	5'- CGC GGA TCCTCCGCCATC AAT TGT GATCCTAATAC -3'	This work	
pET-24a-d(+) pIII N1N2N3 (1-355) R-XhoI	5’- CCGCTCGAG TTAGTGCAGGTTTTC AGAAAAGAGGGA G-3’	This work	

Table 2.2. Antibodies

Antibody	Description	Source/storage
Anti TcpA	Rabbit polyclonal antibody against TcpA C-terminal peptide (residues 174-189)	Ron Taylor/-20^{0}C antibodies box
Anti TcpB	Rabbit polyclonal antibody against TcpB peptide (64-78)	Ron Taylor
Anti ΔN-TcpB	Chicken polyclonal antibodies raised purified ΔN-TcpB	Pacific immunology/-
Anti CTXφ pIII	Rabbit polyclonal antibody against pIII-N2 peptide (residues 186-202)	Pacific immunology/-
Goat anti-rabbit AP-conjugated	Polyclonal raised in goat against rabbit antibodies, alkaline phosphate conjugated	Bio rad/-20^{0}C antibodies box
Goat anti-rabbit gold conjugated	Polyclonal raised in goat against rabbit antibodies, conjugated to 12nm gold particles	Jackson immunoresearch/
Donkey anti-chicken gold label	Polyclonal raised in donkey against chicke antibodies, conjugated to 12nm gold particles	Jackson immunoresearch/

2.2. Preparation of CTXφ pIII constructs

Based on amino acid sequence alignment of CTXφ pIII with M13 pIII, and on structural comparisons between the CTXφ pIII-N1 crystal structure (Ford C., et al. 2012) and the M13 pIII N1 and N1N2 structures. I generated several pIII constructs containing the CTXφ pIII central domain N2 listed in Table 2.3. These constructs were then tested for expression and production of soluble protein. As no soluble proteins were obtained I continued by refolding the largest construct produced. This construct consisted of the entire pIII protein (1-355) with a truncated putative TM helix (last 26 residues of the C-terminal region) Construct 1 (CTXφ pIII-ΔTM), Table 2.3.

Table 2.3. List of CTXφ pIII constructs containing pIII central domain N2 generated tested for expression and solubility

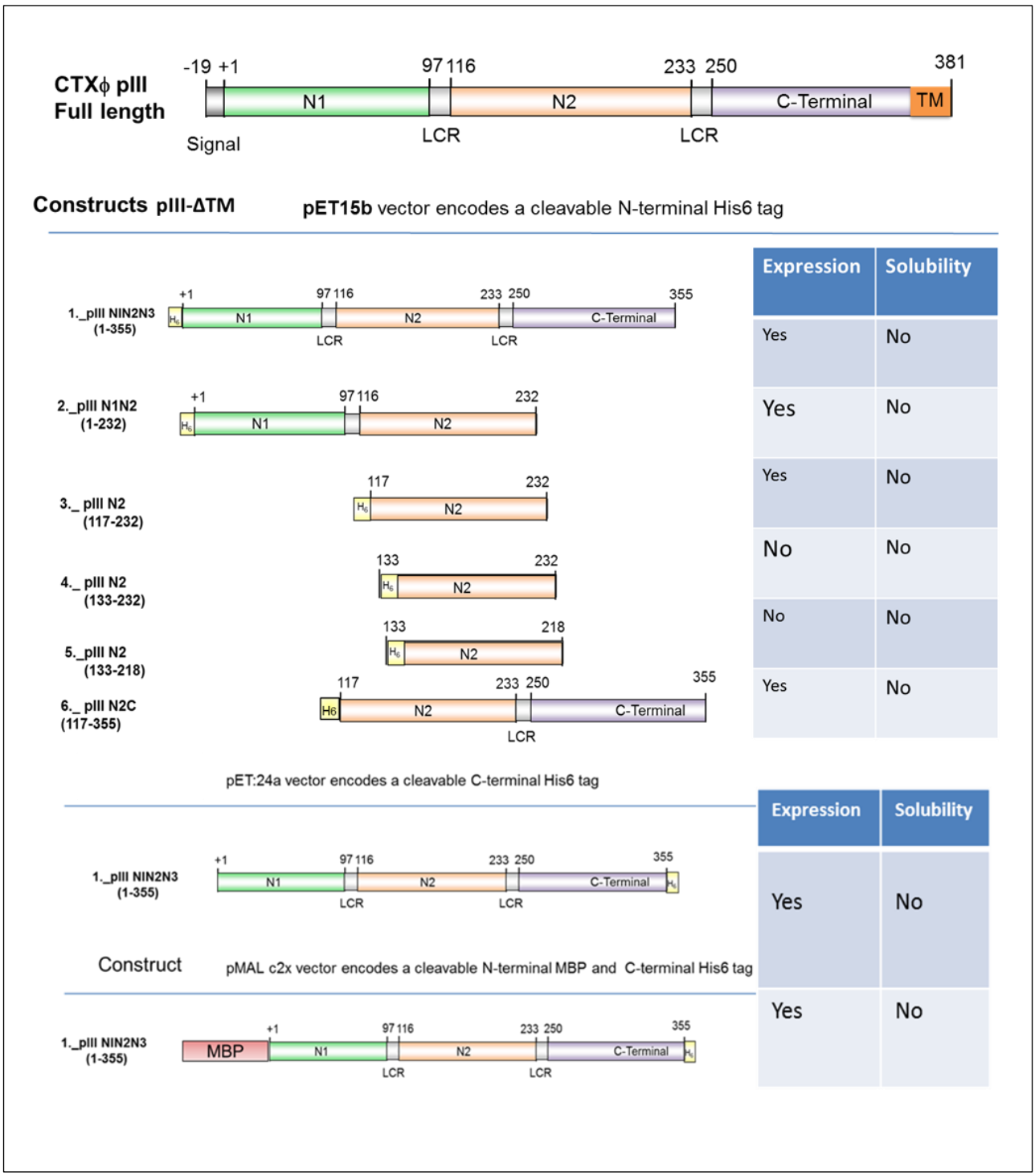

Expression	Solubility
Yes	No
Yes	No
Yes	No
No	No
No	No
Yes	No

Expression	Solubility
Yes	No
Yes	No

2.3. Expression and Purification of pIII-ΔTM and ΔN-TcpB proteins

The gene fragment encoding ΔN-TcpB (residues 23–423, Ng et al., 2016) was PCR amplified with primers TcpB25-vc-fpcr-Nde1 and TcpB25-vc-rpcr-BamH1 from *V. cholerae* wild type strain O395 genomic DNA, followed by digestion with restriction enzymes NdeI and BamHI. The product was ligated into expression vector pET15b (Novagen), which encodes an N-terminal His-tag and linker with a thrombin cleavage site. The gene fragment encoding CTXφ pIII-ΔTM (residues 1–355) was PCR amplified with primers CTXφ pIII N1N2N3(1-355)-F-BamH1 and CTXφ pIII N1N2N3(1-355)-R-NdeI from *V. cholerae* CL101 strain genomic DNA, followed by digestion with NdeI and BamHI and the product was ligated into expression vector pET15b (Novagen), which encodes a His-tag and linker with a thrombin cleavage site. Both constructs were used to transform SHuffle T7 Express lysY Competent *E. coli* (New England Biolabs) by heat shock. Cells were grown overnight in 200 ml of LB broth containing 100 µg/ml Ap at 37 °C shaking at 200 rpm. Ten-ml aliquots of overnight culture were used to inoculate 1 liter of LB-Ap and grown at 37 °C to an optical density at 600 nm (OD_{600}) of ~0.2. Protein expression was induced by the addition of isopropyl β-D-thiogalactopyranoside (IPTG) to 0.4 mM and cells were grown overnight at 19 °C with shaking. Cells were pelleted by centrifugation at 4000 × g for 30 min, the supernatant was discarded, and the pellet was resuspended in lysis buffer (Bis-Tris pH 6.5, 100 mM NaCl, 10% glycerol, 0.1% Tween, 5 mM imidazole) with 10 µg/ml lysozyme and a Complete Protease Inhibitor Mixture tablet (EDTA-free, Roche Applied Science). Cells were incubated in lysis buffer stirring at room temperature for 1 hour and then lysed by sonication. The pIII-ΔTM insoluble

protein was denatured in 6 M guanidine hydrochloride buffer at room temperature for 2 hours. Cellular debris was removed by centrifugation at 40,000 × g for 40 min, and the supernatant was filtered through a 0.45-μm membrane. The filtered supernatant was loaded onto a gravity column containing Ni-NTA beads (Qiagen) for affinity purification using the N-terminal His tag on ΔN-TcpB. The column was washed using 30 column volumes of wash buffer (20 mM Bis-Tris, pH 6.5, 100 mM NaCl). For the pIII-ΔTM construct several urea wash buffers were used with decreasing molar concentrations (M) of urea consisting of 6M urea, 4M urea and 2M urea. Proteins were eluted with 300 mM imidazole. Elution fractions containing the His tag on ΔN-TcpB or pIII-ΔTM were concentrated using a stirred cell concentrator (Amicon) with a 10,000-Da molecular mass cut-off membrane and loaded onto a size exclusion column (HiPrep 26/60 Sephacryl S-100 HR, GE Healthcare). Fractions containing purified protein were concentrated to 15–30 mg/ml, flash-frozen in liquid nitrogen, and stored at −80 °C. To remove the His tag, the purified His tag on ΔN-TcpB (46,000 Da) was incubated at 4 °C for 48 hours with ∼1 unit of thrombin (36,000 Da) per mg protein, after which the protein was loaded onto a Ni-NTA column, which was washed with 3 column volumes with wash buffer (20 mM Bis-Tris, pH 6.5, 100 mM NaCl) to remove undigested protein and free His tag. The non-tagged protein was collected in the flow-through and wash fractions from the Ni-NTA column were concentrated in an Amicon stirred-cell concentrator and loaded onto a size-exclusion column (HiPrep 26/60 Sephacryl S-100 HR, GE Healthcare) to remove the thrombin. Stored protein at -80 °C after flash freeze with liquid nitrogen.

2.4. Inhibition and capture ELISAs

To determine the optimal conditions for the pIII:TcpB binding assays, I first investigated the influence on antibody binding of parameters such as the use of blocking agents, different amounts of coated protein and antibody concentration. A concentration gradient of antibody and/or protein was created and absorbance was measured at 405 nm. Optimal conditions were determined to be those that produced a maximal absorbance signal right before reaching saturation. Optimal parameters were determined to be 10 ug of purified protein per well for the coating step, a dilution of 1/1000 for anti-TcpB and anti-CTXφ pIII primary antibodies (Table 2.2.) and a dilution of 1/500 for alkaline phosphatase conjugated secondary antibody. Dilutions were done in 5% W/V Blotto blocking buffer (1x Tris-buffered saline containing 20% Tween-20, 5% skim milk powder). The wells of a polystyrene microtiter plate were coated with 10 μg ΔN-TcpB or pIII-ΔTM diluted in 1x Tris-buffered saline (1x TBS) in a total volume of 35 μL and incubated overnight at 4°C. The plate was washed three times with 1x Tris-buffered saline containing 20% Tween-20 (1x TBST) and once with TBS and blocked with 200 μl/well of 5% Blotto blocking buffer (TBST, 5% skim milk) for 1 hr at 37 °C. The plate was washed with TBST and incubated with competitor protein, 10 μg/well pIII-ΔTM or ΔN-TcpB in 35 μL of TBS for 30 min at rocking at RT. Control wells that did not required the addition of a competitor molecule were incubated with 35 ul of TBS. The plate was washed three times before adding 35 ul/well of primary antibody (1:1000) diluted in 5% blotto and then incubated at RT while rocking for 2 hours. The plate was washed five times before addition of 35 uL/well of alkaline

phosphatase (AP) conjugated secondary antibody diluted (1:500) in 5% Blotto and incubated for 1 hr rocking at RT. The plate was washed again five times with TBS and incubated for 30 min at RT with 35 µl/well of substrate para-nitrophenylphosphate (pNPP) diluted in AP buffer (100 mM Tris-Cl (pH 9.5), 5 mM $MgCl_2$, 100 mM NaCl). The absorbance (Abs) was measured at 405 nm after 30 minutes.

2.5. Autoagglutination assay

V. cholerae cells were grown in 2 mL LB with antibiotics (Sm, Ap as required) for 2 hours at 37°C in a Ferris wheel rotator and cell concentrations were normalized to OD_{600} of 0.01. Normalized cultures were diluted 1/500 in 3 mL LB (pH 6.5) and grown overnight on a Ferris wheel rotator at 30°C with antibiotics and rhamnose as required. Overnight cultures were allowed to settle at room temperature for 15 minutes, after which the autoagglutination phenotype was assessed visually and the OD_{600} of the culture supernatant was measured. Experiments were performed in triplicate.

2.6. CTXφ Transduction Assays

V. cholerae strains, wild type O395, controls Δ*tcpA*, Δ*tcpB* and mutants Δ*tcpB*+p*tcpB*-E5V, Δ*tcpB*+p*tcpB*-E5Q, used in the infection assays were grown overnight in TCP-inducing conditions, using LB-pH 6.5 incubated in Ferris wheel 60 rpm and 30 ^{o}C for 17 hours. To prepare CTXφ, *V. cholerae* CL101 cells were grown in LB-Km at 37 ^{o}C shaking at 200 rpm overnight. The CL101 strain carries a replicative form of the CTXϕ genome, pCTX-Kmϕ, in which a kanamycin (Km) resistance cassette has been is inserted into the *ctxA* gene, disrupting it. CTX-Kmϕ

are produced by this strain, and infection with CTX-Kmϕ imparts kanamycin resistance onto the tranductants. CL101 cells were removed from the overnight culture by centrifugation at 13,000 rpm for 30 seconds. The supernatant containing the phage was filtered using a 0.2-μm pore filter to remove cells. Phage transduction assays were performed by mixing 100 μl of the filtered supernatant with 100 μl of the various *V. cholerae* strains overnight culture and shaking for 30 min at room temperature. Serial dilutions of the infection mixture were plated on LB-Km agar plates to enumerate the transductants and on LB-Sm plates to enumerate the input bacteria. Cells were grown overnight at 37 °C, and colony-forming units (CFU) were counted. The phage transduction frequency is calculated as the ratio of transductants to input *V. cholerae* cells. For the transfection inhibition assay, the filtered cell supernatant containing CTXφ was mixed with 10 μl 4.7 mM His-ΔN-TcpB (20 mg/ml, 4.7 mM, 10 ul 3 mM bovine serum albumin (20 mg/ml) or with buffer only and incubated at room temperature for 30 min prior to its addition to the *V. cholerae* strains.

2.7. Purification of TCP^{H181A}

V. *cholerae* strain RT4225 was used for TCP purification. This strain has a mutation in *tcpA* encoding a His181Ala substitution (Kirn J. et al. 2000). RT4225 cells were grown on an LB plate containing ampicillin (LB-Amp). A single colony was used to inoculate 2 ml of LB-Amp, which was incubated at 37 °C on a rotary shaker for 30 min. The cell culture was diluted to OD_{600} = 0.01 and 400 μl was used to inoculate 200 ml of LB-Ap, pH 6.5, 0.4 mM IPTG, 100 μg/ml in a 2 L flask, which was incubated at 30 °C for 18 hours shaking at 250 rpm. Four ml of 0.5 M

EDTA (pH 8) and 2 ml of 0.1 M histidine-HCl were added to the culture, which was centrifuged at 5000 x*g* for 15 minutes at 4 °C to pellet cells. The supernatant was centrifuged again at 5000 x*g* for 10 minutes at 4 °C to pellet residual cells. After transferring the supernatant to new tubes, solid ammonium sulfate ($AmSO_4$) was added to 10% saturation and the solution was incubated at 4 °C for 2 hours on a rocker. The solution was centrifuged at 10,000 x*g* for 30 minutes at 4°C to remove contaminants, and $AmSO_4$ was added to the supernatant 30% saturation. The solution was incubated at 4°C for one hour on the rocker then centrifuged at 10,000 x*g* for 30 min at 4°C to pellet the pili. The pellet was resuspended in 200 µl of PBS containing 10 mM EDTA and dialyzed using a 3500 kDa molecular weight cut-off membrane against precooled PBS, 10 mM EDTA.

2.8. Negative staining and immunogold TEM imaging

V. *cholerae* cells were grown under TCP-expressing conditions and TCP were purified as described in 2.7. Carbon-coated grids (CF-300, Electron Microscopy Science) were inverted on top of a 25 µL drop of sample on Parafilm and incubated for 15 minutes. Following incubation, grids were transferred to drops of Tris-buffered saline with 0.1% Tween (TBST). Grids were then stained with 3% uranyl acetate and imaged on a Hitachi 8100 STEM operating at 120 kEv or on a Tecnai F20 FEG STEM at 200 kEv.

For immunogold labeled samples, grids were inverted on top of a 25 µl drop of overnight cell culture or purified TCP on Parafilm in a humidified chamber to prevent evaporation and incubated at 30°C for 10 min. Following incubation, grids were transferred to 25 µL drops of fixative (4% paraformaldehyde/0.2%

glutaraldehyde in 0.2 M sodium cacodylate pH 7.4) for 1 hour. Purified TCP were not fixed. The grids were washed with TBST and blocked for 1 hour in TBST containing 2% W/V bovine serine albumin (BSA) in TBST. Samples were incubated with primary chicken antibody raised against purified ΔN-TcpB protein (1:500 dilution in TBST 2% BSA), washed in TBST, and then incubated for 30 minutes with 12 nm gold-conjugated anti-chicken secondary antibody (1:500 dilution in TBST 1% BSA) (Jackson Immunoresearch, Electron Microscopy Sciences). The final wash in TBST was followed by staining with 3% uranyl acetate for 1 minute.

2.9. Statistical analysis

CTXφ phage relative infectivity was measured by counting colony forming units (CFUs). Phage transduction results shown are averages of three separate experiments, the mean value of CFUs observed in the infection of wild type *V. cholerae* cells using phage only was set to 100 percent. Error bars represent the standard error of the mean.Relative infectivity values that differed between the infection of wild type *V. cholerae* cells with phage only and addition of a competitor molecule or *V. cholerae* variant with $p < 0.05$, determined using the Wilcoxon-Mann-Whitney U test, are considered statistically significant.

ELISA results shown are averages of three separate experiments. Error bars represent the standard error of the mean. Absorbance 405 nm values that differed between control and variant with $p < 0.05$; determined using the Wilcoxon-Mann-Whitney U test, are considered statistically significant.

Chapter 3. Results

3.1. Blocking of CTXφ phage infection by soluble TcpB and anti-TcpB antibodies

To investigate the role of TcpB in CTXφ infection, I tested whether soluble TcpB or antibodies directed to TcpB residues 64-78 might block phage interaction with TCP. Phage transduction assays were performed in various *V. cholerae* strains in the absence or present of (i) purified soluble TcpB recombinantly expressed without the N-terminal 28-amino acid polymerization domain (ΔN-TcpB, Ng et al. 2016) or (ii) antibodies directed against a TcpB residues 64-78 on the C-globular domain. *V. cholerae* strains used in the transduction assays were grown overnight under TCP-inducing conditions. To prepare CTXφ phage for infection, *V. cholerae* CL101 cells were grown in LB-Km at 37 °C on the shaker overnight. CL101 cells produce CTX-Km in which the *ctxA* gene is replaced with the Km resistance marker (Waldor and Mekalanos, 1996). Transduction assays were performed by mixing supernatant containing phage with *V. cholerae* overnight culture and incubating for 30 min at room temperature. For the blocking assays, phage were pre-incubated with ΔN-TcpB or *V. cholerae* were pre-incubated with anti-TcpB antibody prior to combining the phage and *V. cholerae*. Serial dilutions of the infection mixture were plated on LB-Km agar plates to enumerate the transductants and on LB-Sm plates to enumerate the input bacteria. Cells were grown overnight at 37 °C, and cfus were counted. As shown previously (Waldor and Mekalanos, 1996; Kirn et al. 2000; Gao et al. 2016) *V. cholerae* Δ*tcpA* and Δ*tcpB* strains show no transduction with CTX-Km (Fig. 3-1). This is expected for Δ*tcpA*, as deletion of the major pilin subunit results in complete loss of piliation. However, the Δ*tcpB* strain makes some pili,

from 1-10 % of the WT strain (Ng D. et al 2016), yet no transductants are observed despite the extreme sensitivity of this assay, suggesting that TcpB, in addition to the pilus, is critical for CTXφ infection. Transduction was restored to WT levels for the Δ*tcpB* mutant complemented with a plasmid carrying the *tcpB* gene, p*tcpB*. WT *V. cholerae* cells infected with CTXφ that were preincubated with ΔN-TcpB showed a 90% reduction in transduction frequency, and cells preincubated with anti-TcpB antibody showed a 95% reduction. In contrast, neither soluble albumin nor an unrelated antibody, anti-CofJ, had any effect on transduction frequencies. These results suggest that TcpB is present on the pilus and is involved in interaction with CTXφ to facilitate uptake.

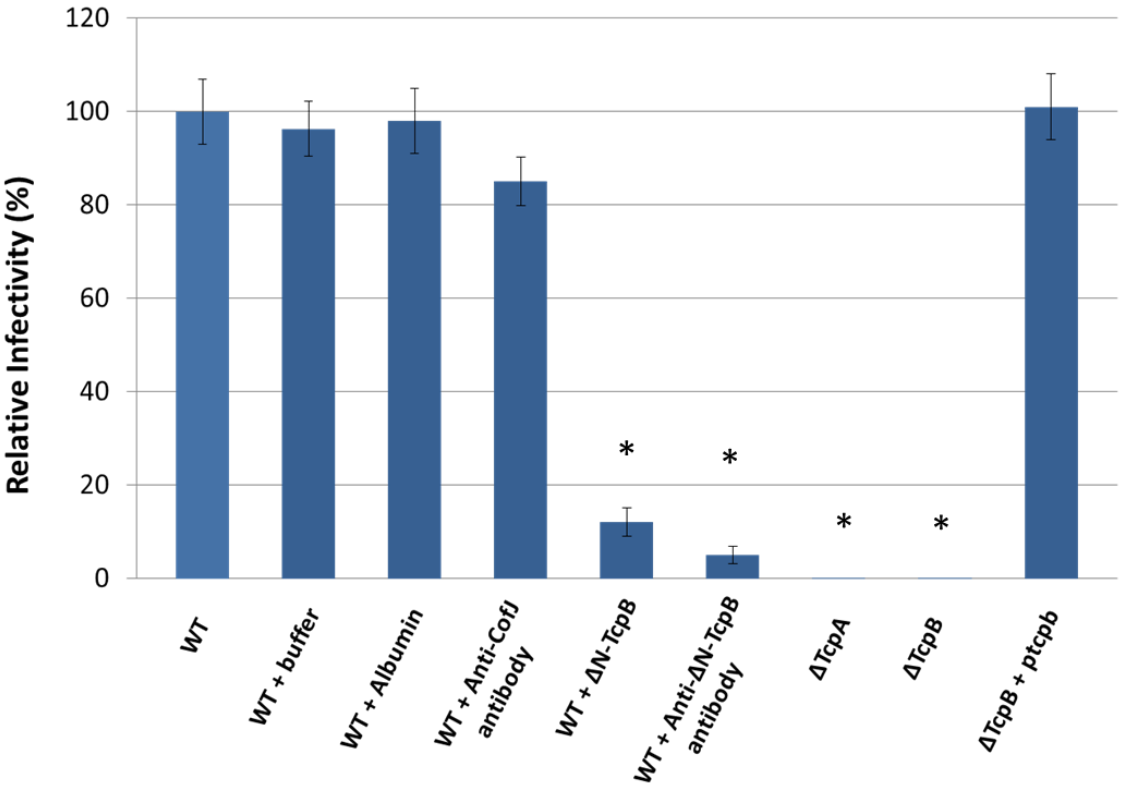

Figure 3-1. Soluble ΔN-TcpB and anti-TcpB antibody block CTXφ phage infection of *V. cholerae* cells. Buffer, albumin and an unrelated antibody, anti-CofJ antibody, were used as controls for blocking phage infection of cells. Soluble ΔN-TcpB and anti TcpB antibody reduce phage infection by 90% and 95% respectively. CTXφ phage does not infect *V. cholerae* Δ*tcpA* strain, which makes no pili, nor does it infect *V. cholerae* Δ*tcpB* despite this strain producing low levels of pili.
Results shown are averages of three separate experiments, the calculated CFUs mean value in the infection of wild type *V. cholerae* cells using phage only was set to 100 percent. Error bars represent the standard error of the mean.
* indicates statistically significant differences between the infection of wild type *V. cholerae* cells with phage only and addition of a competitor molecule or *V. cholerae* mutant. *$p < 0.05$; Wilcoxon-Mann-Whitney U test.

3.2. Soluble ΔN-TcpB binds to immobilized CTXφ tip protein pIII-ΔTM

Having shown that TcpB is involved in CTXφ infection, I used ELISA to test whether TcpB might interact directly with CTXφ pIII, the tip-associated protein that binds to TCP (Heilpern & Waldor M.K., 2003). CTXφ pIII was expressed recombinantly in a form lacking only its C-terminal transmembrane segment (amino acids 355-381, pIII-ΔTM). Microtiter plates were coated with CTXφ pIII-ΔTM, or with the positive control protein TcpB or negative controls TcpA and bovine serum albumin. After blocking unbound sites of the plates with BSA, increasing amounts of soluble ΔN-TcpB was added to the wells as specified (Fig. 3-2). Following incubation the plates were washed and rabbit anti-TcpB antibody was added, followed by anti-rabbit antibody conjugated to alkaline phosphatase (AP). Substrate, pNPP, was added and samples were read at Abs_{405}. Abs_{405} readings show a gradual increase in signal strength corresponding to increasing ΔN-TcpB for the pIII-bound wells, with values approaching that of TcpB coated directly on the plate, indicating that TcpB binds to immobilized CTXφ pIII.

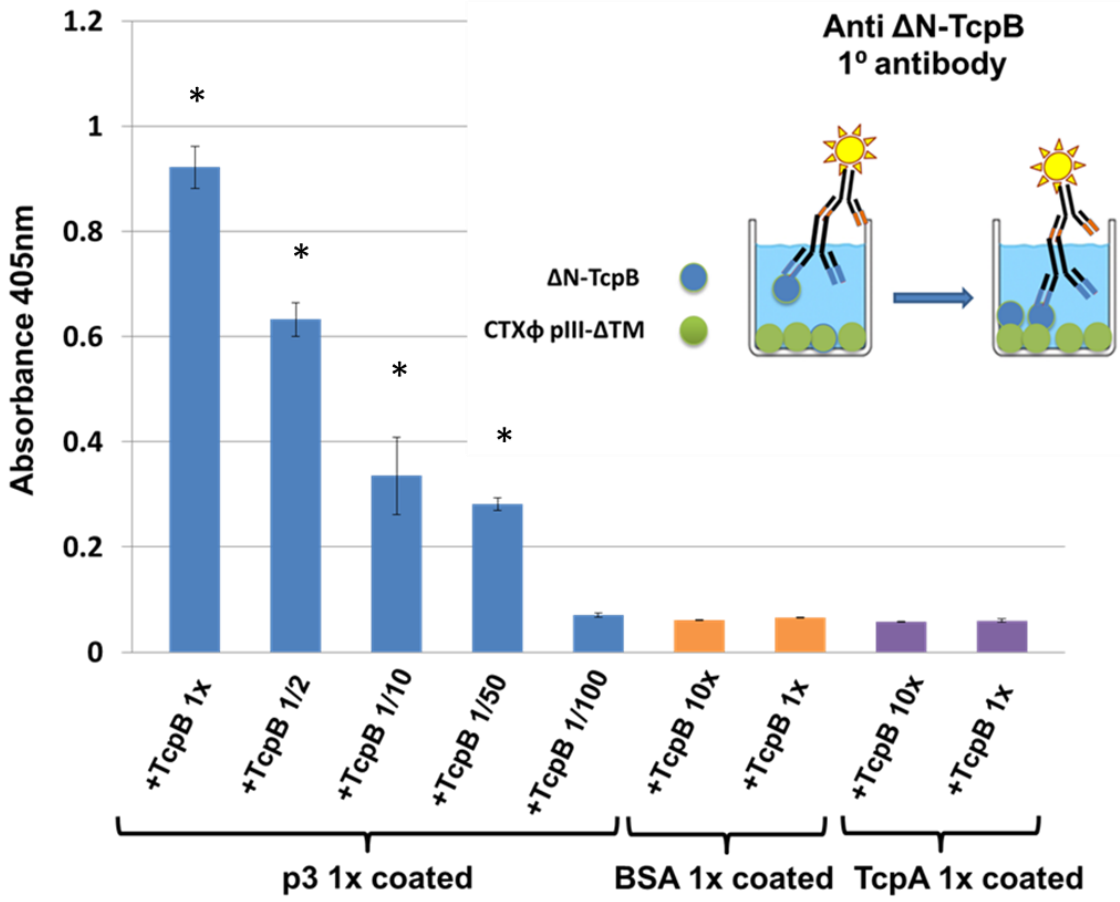

Figure 3-2. **Soluble ΔN-TcpB binds to immobilized CTXφ tip protein pIII**. The wells of a polystyrene microtiter plate were coated with 7.5 μM of CTXφ pIII-ΔTM (1-355) shown as p3 1x. Bovine serum albumin (BSA) and ΔN-TcpA were used as controls to test the immobilized pIII capture specificity. + TcpB 1x corresponds to 7.5 μM of soluble ΔN-TcpB added to coated wells. ΔN-TcpB was added at varying concentrations. The primary antibody used in all wells was anti-ΔN-TcpB antibody. Results shown are averages of three separate experiments. Error bars represent the standard error of the mean.
*$p < 0.05$; Wilcoxon-Mann-Whitney U test.

3.3. Soluble CTXφ pIII binds to immobilized ΔN-TcpB

In a reciprocal experiment I tested the ability of CTXφ pIII-ΔTM to bind to immobilized TcpB. Microtiter wells were coated with ΔN-TcpB or positive control pIII or negative controls TcpA and BSA. After blocking, soluble CTXφ pIII-ΔTM was added to the wells. Following incubation the plates were washed and the wells probed with anti-CTXφ pIII antibody and anti-rabbit secondary antibody conjugated to alkaline phosphatase. Abs_{405} values decreased with decreasing concentrations of CTXφ pIII (Fig. 3-3) in the TcpB-bound plated but not the BSA- or TcpA -bound plates, demonstrating a direct interaction between soluble CTXφ pIII and immobilized TcpB.

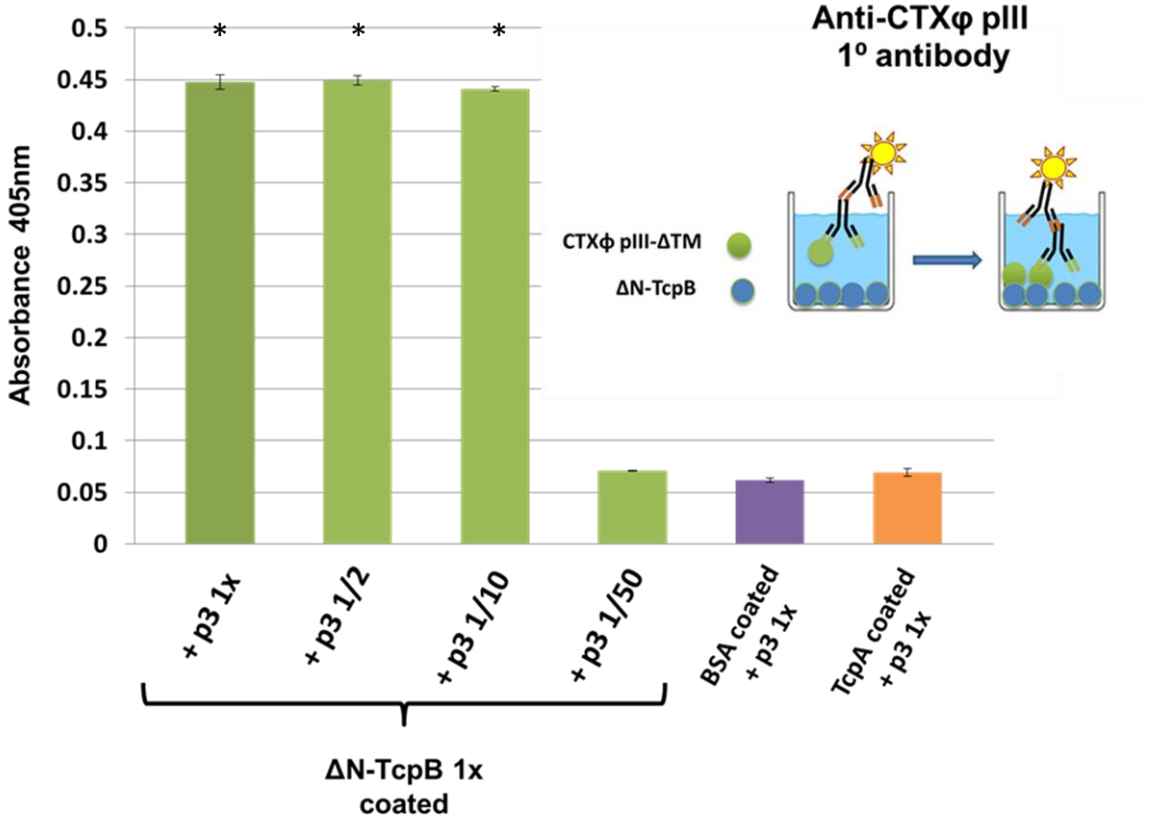

Figure 3-3. Soluble CTXφ pIII-ΔTM binds to immobilized ΔN-TcpB. The wells of a polystyrene microtiter plate were coated with 7.5 μM soluble ΔN-TcpB. BSA and ΔN-TcpA were used as controls. P3 1x corresponds to 7.5 uM of CTXφ pIII-ΔTM (1-355). The primary antibody used in all wells was anti-CTXφ pIII-ΔTM antibody. OD readings show a signal corresponding to the presence of CTXφ pIII. However, in comparison with the reciprocal experiment, here the signal strength is reduced and does not vary concomitantly with the changes in amount soluble protein added.
Results shown are averages of three separate experiments. Error bars represent the standard error of the mean.
*$p < 0.05$; Wilcoxon-Mann-Whitney U test.

3.4. Soluble CTXφ pIII-ΔTM competes with anti-TcpB antibody for binding to immobilized ΔN-TcpB

To further test the TcpB and CTXφ pIII binding, a competition ELISA was performed to test the ability of pIII to compete with anti-TcpB antibody for binding to immobilized TcpB. Microtiter wells were coated with ΔN-TcpB. After blocking, increasing amounts of soluble CTXφ pIII-ΔTM were added to the wells. Following incubation the plates were washed and the wells probed with anti-TcpB antibody and AP-conjugated anti-rabbit secondary antibody. Abs_{405} values decrease with increasing amounts of pIII-ΔTM (Fig. 4), suggesting that pIII binding to immobilized TcpB prevents anti-TcpB from binding. A reciprocal experiment was performed with immobilized pIII-ΔTM, but in this case we did not observe competition of anti-pIII antibody by ΔN-TcpB for binding to pIII (Fig. 3-4). This may mean that both anti-pIII antibody and TcpB simultaneously bind to immobilized pIII or that the anti-pIII antibody binds to pIII-ΔTM with a much higher affinity, competing off TcpB.

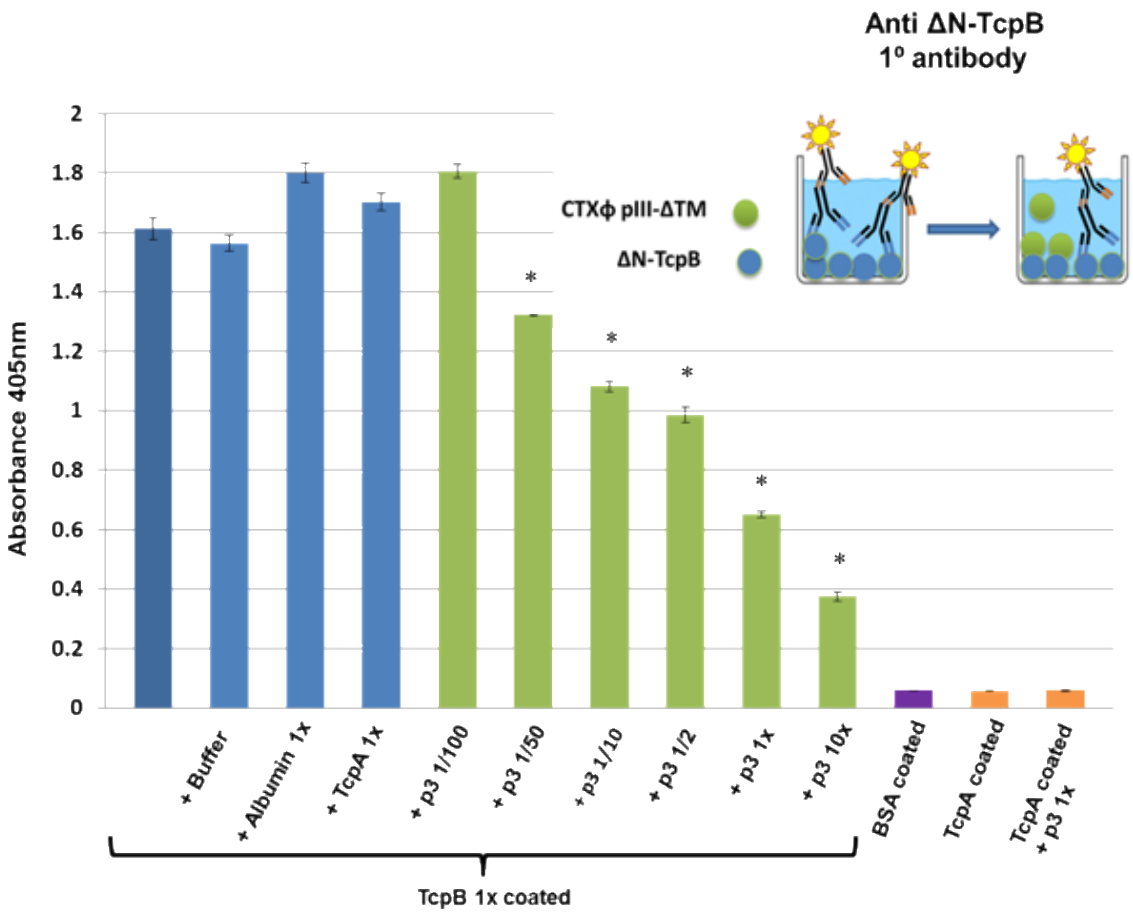

Figure 3-4. Soluble CTXφ pIII competes with anti-TcpB antibody for binding to immobilized ΔN-TcpB. The wells of a polystyrene microtiter plate were coated with 7.5 μM of ΔN-TcpB, shown as TcpB 1x. Coated wells with BSA and TcpA were used as controls to test the antibody specificity. Albumin and ΔN-TcpA were added as antibody competitive controls. + p3 1x corresponds to 7.5 μM of soluble CTXφ pIII-ΔTM. pIII-ΔTM was added at different concentrations. The primary antibody used in all wells was anti ΔN-TcpB antibody. Results shown are averages of three separate experiments. Error bars represent the standard error of the mean.
*$p < 0.05$; Wilcoxon-Mann-Whitney U test.

3.5. The *V. cholerae* minor pilin TcpB is located at the tip of the toxin coregulated pilus (TCP)

We proposed previously that TcpB is located at the tip of the pilus where it initiates pilus assembly (Ng et al., 2016). There is substantial evidence supporting tip localization for other minor pilins (Korotkov and Hol, 2008; Giltner et al. 2010; Korotkov et al., 2012; Kolappan et al., 2015; Ng et al., 2016) but this has not been demonstrated directly. My data showing that the phage tip protein pIII interacts with the *V. cholerae* minor pilin TcpB further supports tip localization for TcpB. To show this directly, we immunogold labeled TcpB on purified pili and imaged them by transmission electron microscopy (TEM). Pili were purified from *V. cholerae* strain RT4225 (Fig. 3-5) (Kirn et al 2000), in which the major pilin, TcpA, has an alanine substitution in a surface-exposed residue, His181 (TCP^{H181A}). This single amino acid change disrupts pilus:pilus interactions that lead to bacterial aggregation which normally occurs in wild type cells (Fig. 3-5IV). The non-bundled pili produced by *V. cholerae* RT4225 are shed into the culture supernatant during overnight growth, where they can be separated from the cells by centrifugation and purified by ammonium sulphate precipitation. This process provides substantial quantities of non-bundled pili for immunogold labeling. I used an anti-TcpB polyclonal chicken primary antibody raised against ΔN-TcpB protein and a gold labeled donkey anti-chicken secondary antibody to visualize TcpB on the pili. To quantitatively assess the association of TcpB on pilus tips, pili were examined in 23 randomly selected TEM visual fields. Sixty-six pili were observed in total and 45 of them (68%) contained at least one gold particle at one of the pilus ends. These data represent direct evidence that TcpB is present at the tip of TCP and supports the previously

proposed model by Ng et al. where TcpB is the first pilin in the growing pilus, consistent with its role in initiating pilus assembly.

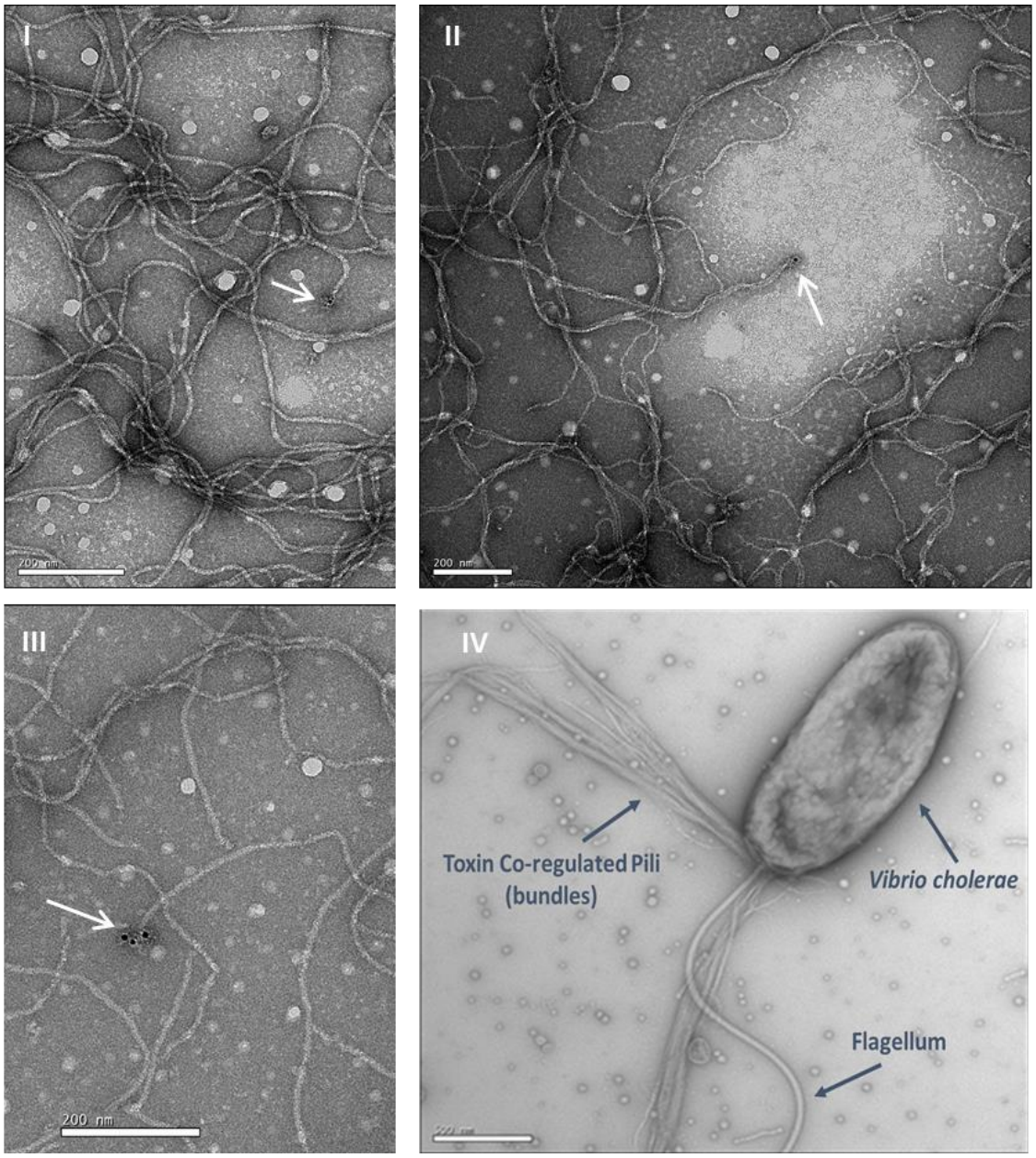

Figure 3-5 TcpB localizes at the tip of purified TCP^{H181A}. (I,II,) shows images of immunogold labelled purified pili with a gold particle at the ends of pili.**(III)** Shows three gold particles at the end of purified pili. White arrows point to gold particles at pili tips. **(IV)** Shows WT *V. cholerae* cells expressing bundled TCP (blue arrows) and a single flagella. Images were obtained using a STEM-Tecnai G2.

3.6. TcpB-mediated pilus retraction is a necessary step in phage uptake

We hypothesize that once a tip to tip interaction occurs between CTXφ and TCP, the similar diameters of the phage and the pilus allow it to be transported across the outer membrane via TCP retraction as if it were an extension of the pilus. Pilus retraction is initiated by TcpB, which in addition to initiating pilus assembly by forming at its tip, also appears to insert into the growing pilus as if it were a major pilin, stalling pilus assembly by blocking passage of the pilus through the outer membrane secretin channel or by preventing addition of new major pilin subunits. When pilus assembly is stalled, the last major pilin added to the growing pilus will translocate from the base of the pilus back into the inner membrane, one subunit at a time. Thus, we propose that phage uptake, as well as phage binding, occurs in a TcpB dependent manner.

In order to test this hypothesis we utilized our TcpB Glu5 variants in phage transduction assays. For these variants, the *V. cholerae* Δ*tcpB* strain was complemented with p*tcpB* mutants encoding the Glu5 substitutions aspartate, glutamine and valine. All TcpB Glu5 variants produce pili at greater than wild type levels yet TcpF secretion and autoagglutination are both impaired in these mutants, to a degree corresponding to the nature of the substitution: the most conservative change, Glu5Asp, has only mild effect on TcpF secretion and autoagglutination, whereas the most dramatic change, Glu5Val, has the severest effect (Ng 2016). In this earlier study, the mutation encoding the Glu5Val substitution was introduced into the *tcpB* gene within the *V. cholerae* chromosome I to ensure that the TcpB-E5V variant was produced in endogenous levels. This mutant was shown using the

micropillars assay to be completely defective for pilus retraction (Ng 2016). These results are consistent with TcpB-E5V being able to initiate pilus assembly but the variant is not able to incorporate into the growing pilus to stall assembly, triggering retraction, which is required for TcpF secretion and autoagglutination.

We similarly observed a gradient of impairment in phage uptake depending on the nature of the Glu5 substitution: the most conserved change, to the negatively charged aspartate (E5D) showed a 5% reduction compared to the WT strain; the Glu5Gln (E5Q) substitution, which results in loss of the negative charge but retains polarity, showed a 20% transduction in frequency reduction; and the Glu5Val corresponding to the most divergent substitution resulted in a dramatic 99% reduction in phage transduction to almost undetectable levels (Fig. 3-6). These data suggest that TCP retraction is necessary for efficient CTXφ phage uptake.

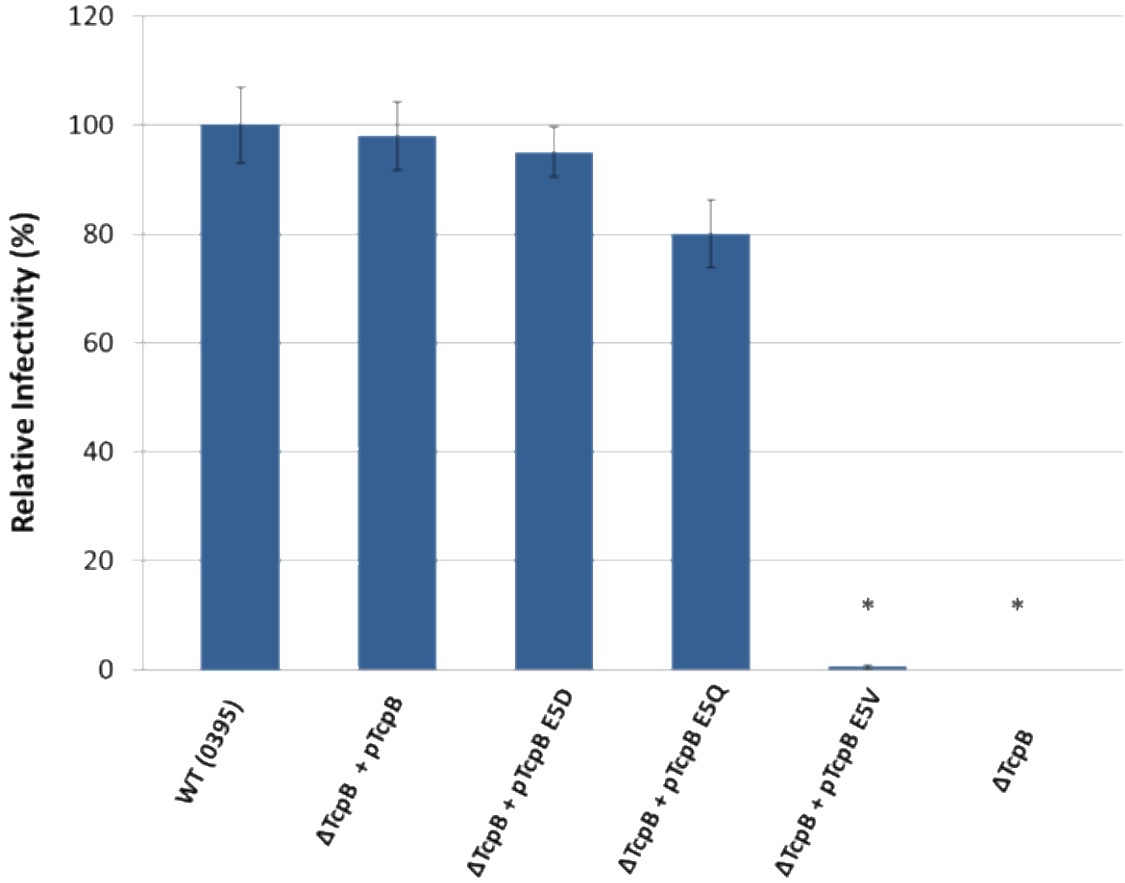

Figure 3-6. Retraction is necessary for efficient CTXφ phage uptake. *V. cholerae* strains, wild type O395, controls: CTXφ uptake is undetectable in the Δ*tcpA* and Δ*tcpB* strains (shown in Figure 3-1). ΔtcpB + p*tcpB* contains a plasmid that overexpresses TcpB. CTXφ uptake in this strain occurs at similar levels as wild type strain.

Results shown are averages of three separate experiments, the mean value of CFUs observed in the infection of wild type *V. cholerae* cells using phage only was set to 100 percent. Error bars represent the standard error of the mean.

* indicates statistically significant differences between the infection of wild type *V. cholerae* cells with phage only and addition of a competitor molecule or *V. cholerae* mutant. *$p < 0.05$; Wilcoxon-Mann-Whitney U test.

Chapter 4. Discussion

My results support a TcpB:CTXφ pIII interaction and suggest a tip to tip interaction between phage and the pilus. I demonstrate that blocking TcpB with bound antibody and that using soluble TcpB as a competitor reduces phage transduction significantly, which suggests a TcpB:CTXφ phage interaction. I further show that purified recombinant soluble TcpB binds to immobilized CTXφ pIII and vice versa via ELISA. Furthermore, using immunogold labeling, I showed that TcpB in fact localizes at the tip of Toxin co-regulated pili. Finally, by using a *V. cholerae* TcpB Glu5 variants, I provide evidence that supports our premise that phage uptake is facilitated via TCP retraction.

Taken together, my results allow us to propose a revised working model for CTXφ phage infection in *V. cholerae* (Fig. 4-1). In this model, CTXφ binds to TCP, in a tip to tip manner, in which CTXφ pIII binds to TcpB at the tip of TCP. CTXφ is then taken up via TCP retraction into the periplasmic domain and CTX pIII-N1 interacts with TolA (Ford et al. 2012; Karlsson et al. 2003) to facilitate shedding of its protein coat in the inner membrane and release phage DNA into the cytoplasm (Davis and Waldor, 2003). Tip interactions among Ff coliphage and F-pilus have been proposed (Armstrong et al. 1981; Stengele et al., 1990) but never shown. Thus, my model represents an important advance understanding CTXφ phage uptake.

As we propose that a CTX pIII:TcpB interaction is necessary for efficient phage uptake, it is possible that other CTX phage:pilus interactions are also necessary for phage uptake. I found that in the presence of the molecular competitor anti-TcpB, phage infection of wild type *V. cholerae* can still be detected. It is conceivable that additional interactions, such as lateral interactions between the filamentous phage and the pilus

may also contribute to phage uptake. These lateral interactions may occur as an initial recognition step before a tip to tip interaction. This seems reasonable since these lateral interactions would be much more likely to occur due to the large surface area compared to the very specific TcpB:pIII interaction.

Additionally, phage transduction occurs, albeit at low levels, in the tcpB-E5V mutant. There are several possible explanations for this observation. One is that TcpB-E5V can incorporate into the pilus to induce retraction, but does so inefficiently because it does not have the attractive force between Glu5 and the N1+ of the last major pilin added in the growing pilus. Another possibility is that phage uptake can occur independently of TcpB mediated retraction, although less efficiently. Ng et al. proposed that pilus retraction in E5V mutants can occur spontaneously in a TcpB-independent manner when pilus assembly becomes stalled, although infrequently. A third possibility is that the phage:pilus interaction itself provides a stimulus for retraction. It seems reasonable that a CTXφ phage:pilus interaction could cause tension-induced changes in the conformation of TCP that trigger retraction. Similarly to *Neisseria meningitides* and *N. gonorrhoeae*, in which their more complex T4a exhibit conformational changes upon stretching that reduce pilus width and expose, previously hidden PilA epitopes (Biais et al. 2010). Additionally, Persat et al showed that the T4a pili in Pseudomonas aeruginosa can mechanochemically regulate virulence factors. They used the bacterial two-hybrid system (BACTH) to show that the major pilin, PilA, interacts with the chemosensory protein PilJ of the Chp system. They proposed that once T4P surface attachment occurs, PilJ senses tension-induced changes of PilA which in turn enhances a positive feedback loop via the Chp System that drives pilus retraction using retraction ATPase.

Given that the more simplistic TCP system in *V. cholerae* lacks a retraction ATPase, it seems plausible that non-TcpB dependent retraction occurs due a change in the pilus structure conformation upon interaction with a surface or CTXφ phage. There is yet to be identified a chemosensory protein like PilJ in *V. cholerae*. However, it seems reasonable that there are chemosensory systems in place that can sense a change in conformation of T4b pili and in turn drive pilus retraction in the absence of a wild type minor pilin.

Another of my thesis objectives is to investigate the localization of the *V. cholerae* minor pilin, TcpB, within the toxin co-regulated pilus (TCP). Using immunogold labeling, I showed that TcpB localizes at the tip of H181A TCP purified pili. Some purified pili had more than one gold particle at the tip. The presence of gold clusters at the pilus tip could be due the usage of a polyclonal antibody raised against the purified ΔN-TcpB protein to detect the minor pilin. It is possible that several antibodies can bind to distinct epitopes of one single minor plin within its pilus tip associated conformation. In the other hand, gold clusters could merely be an artifact of the immunogold labelling protocol; in which the gold conjugated antibodies can associate with each in a non-specific manner and at the same time still be able to label TcpB at the pilus tip. In any case, these results show definitively the presence of TcpB at the tip of TCP. To our knowledge, these results represent the first direct demonstration of a minor pilin at the tip of a T4P.

Overall, my results support the hypothesis that the *V. cholerae* minor pilin, TcpB localizes at the tip of the pilus and it is the receptor of CTXφ phage tip protein pIII. Given the similarities between the Type IVb pili like *V. cholerae* TCP and ETEC CFA/III and the Type IVa pili and the T2S pseudopili, it seems likely that the minor pilins in

these other systems also locate at the pilus tips. Furthermore, it seems reasonable that minor pilins in other T4P systems also serve as receptors for filamentous phages which are then taken up via pilus retraction.

Currently there is no urgent need for new antibiotics against *V. cholerae*. Cholera is a self-limiting disease and complete recovery is accomplished by treating the symptoms. Nonetheless, our *V. cholera* model would serve as a proof of concept in our quest to use T4P as a novel antibiotic delivery method for Gram negative bacteria. My results are of particular interest in the search for new antimicrobial targets and novel antibiotic delivery methods for Gram negative bacteria. We could take advantage of the T4P pilus retraction system and the filamentous phage uptake mechanism by targeting TcpB or other minor pilins at pili tips and deliver drugs into the periplasm space and neutralize/kill the cell.

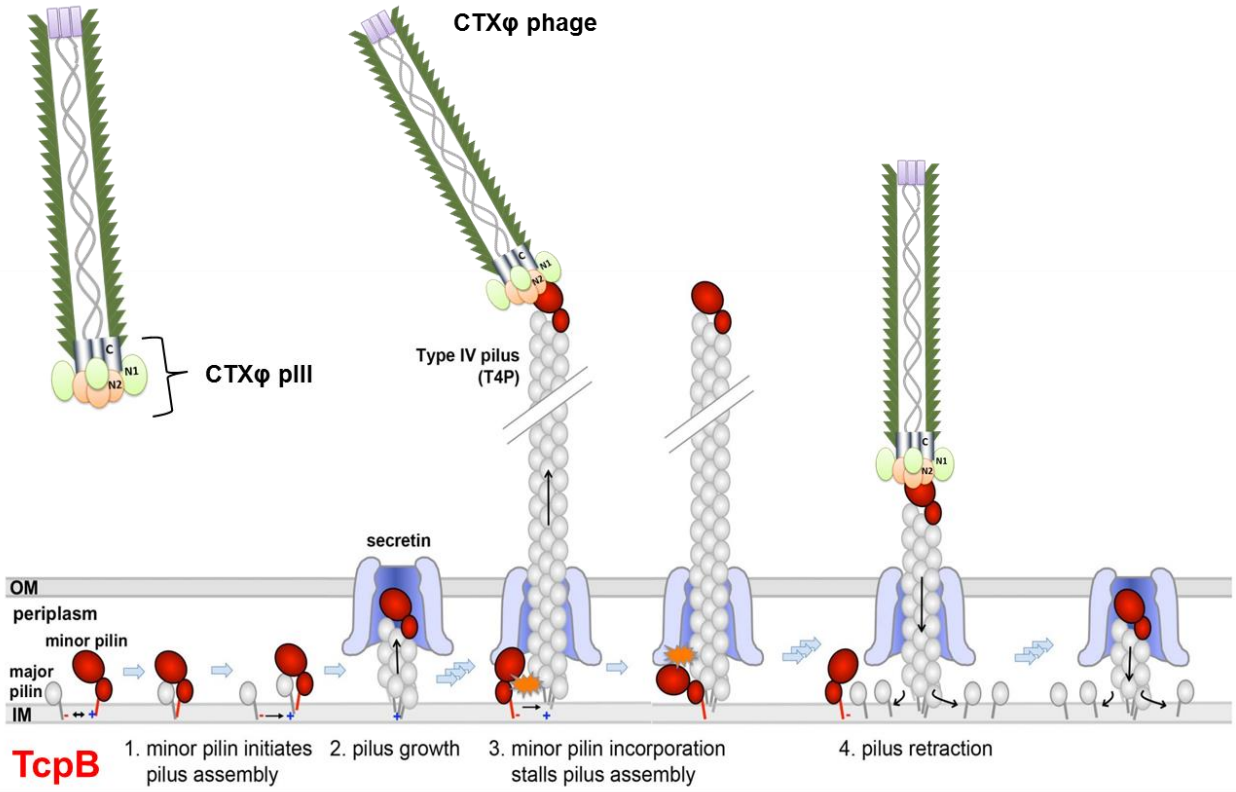

Figure 4-1. **Model proposed for CTXφ uptake by *V. cholera*.** The minor pili TcpB is shown in Red. Major pilin, TcpA, is shown in grey. It still remains unclear whether the minor pilin incorporates and is extruded along an assembling filament to induce retraction, or simply incorporates at the base of a growing filament to induce retraction without extrusion.

References

Anantha, R. P., Stone, K. D., & Donnenberg, M. S. (1998). Role of BfpF, a Member of the PilT Family of Putative Nucleotide-Binding Proteins, in Type IV Pilus Biogenesis and in Interactions between Enteropathogenic *Escherichia coli* and Host Cells. *Infection and Immunity*, *66*(1), 122–131.

Armstrong, J., Perham, R. N., & Walker, J. E. (1981). Domain structure of bacteriophage fd adsorption protein. *FEBS letters*. 135(1), 167-172.

Basu, A., Mukhopadhyay, A. K., Garg, P., Chakraborty, S., Ramamurthy, T., Yamasaki, S., Nair, G. B. (2000). Diversity in the arrangement of the CTX prophages in classical strains of *Vibrio cholerae* O1. *FEMS Microbiology Letters*, *182*(1), 35–40.

Barbas, C. F., Burton, D. R., Scott, J. K., & Silverman, G. J. Phage display: a laboratory manual. (2001). Plainview, NY, Cold Spring Harbor Laboratory Press

Beck, E., & Zink, B. (1981). Nucleotide sequence and genome organisation of filamentous bacteriophages f1 and fd. *Gene*, *16*(1–3), 35–58.

Bentzmann, S. de, Aurouze, M., Ball, G., & Filloux, A. (2006). FppA, a Novel *Pseudomonas aeruginosa* prepilin peptidase involved in assembly of Type IVb pili. *Journal of Bacteriology*, *188*(13), 4851–4860.

Berche, P., Poyart, C., Abachin, E., Lelievre, H., Vandepitte, J., Dodin, A., & Fournier, J.-M. (1994). The novel epidemic strain 0139 Is closely related to the pandemic strain 01 of *Vibrio Cholerae*. *The Journal of Infectious Diseases*, *170*(3), 701–704.

Bernard, S. C., Simpson, N., Join-Lambert, O., Federici, C., Laran-Chich, M.-P., Maïssa, N., … Bourdoulous, S. (2014). Pathogenic *Neisseria meningitidis* utilizes CD147 for vascular colonization. *Nature Medicine*, *20*(7), 725–731.

Berry, J.-L., & Pelicic, V. (2015). Exceptionally widespread nanomachines composed of type IV pilins: the prokaryotic Swiss Army knives. *FEMS Microbiology Reviews*, *39*(1), 1–21.

Biais, N., Higashi, D. L., Brujić, J., So, M., & Sheetz, M. P. (2010). Force-dependent polymorphism in type IV pili reveals hidden epitopes. *Proceedings of the National Academy of Sciences*, *107*(25), 11358–11363.

Biais, N., Ladoux, B., Higashi, D., So, M., & Sheetz, M. (2008). Cooperative retraction of bundled Type IV pili enables nanonewton force generation. *PLOS Biology*, *6*(4), e87.

Bose, N., & Taylor, R. K. (2005). Identification of a TcpC-TcpQ outer membrane complex involved in the biogenesis of the toxin-coregulated pilus of *Vibrio cholerae. Journal of Bacteriology*, *187*(7), 2225–2232.

Brissac, T., Mikaty, G., Duménil, G., Coureuil, M., & Nassif, X. (2012). The Meningococcal minor pilin PilX Is responsible for Type IV Pilus conformational changes associated with signaling to endothelial cells. *Infection and Immunity*, *80*(9).

Brossay, L., Paradis, G., Fox, R., Koomey, M., & Hébert, J. (1994). Identification, localization, and distribution of the PilT protein in *Neisseria gonorrhoeae*. *Infection and Immunity*, *62*(6), 2302–2308.

Bubien, J. K., Jope, R. S., & Warnock, D. G. (1994). G-proteins modulate amiloride-sensitive sodium channels. *Journal of Biological Chemistry*, *269*(27), 17780–17783.

Burrows, L. L. (2005). Weapons of mass retraction. *Molecular Microbiology*, *57*(4), 878–888.

Carroll, P. A., Tashima, K. T., Rogers, M. B., DiRita, V. J., & Calderwood, S. B. (1997). Phase variation in tcpH modulates expression of the ToxR regulon in Vibrio cholerae. *Molecular Microbiology*, *25*(6), 1099–1111.

Chami, M., Guilvout, I., Gregorini, M., Rémigy, H. W., Müller, S. A., Valerio, M., … Bayan, N. (2005). Structural Insights into the Secretin PulD and Its Trypsin-resistant Core. *Journal of Biological Chemistry*, *280*(45), 37732–37741.

Champion, G. A., Neely, M. N., Brennan, M. A., & DiRita, V. J. (1997). A branch in the ToxR regulatory cascade of *Vibrio cholerae* revealed by characterization of toxT mutant strains. *Molecular Microbiology*, *23*(2), 323–331.

Chang, Y.-W., Kjær, A., Ortega, D. R., Kovacikova, G., Sutherland, J. A., Rettberg, L. A., … Jensen, G. J. (2017). Architecture of the *Vibrio cholerae* toxin-coregulated pilus machine revealed by electron cryotomography. *Nature Microbiology*, *2*(4), nmicrobiol2016269.

Cisneros, D. A., Bond, P. J., Pugsley, A. P., Campos, M., & Francetic, O. (2012). Minor pseudopilin self-assembly primes type II secretion pseudopilus elongation. *The EMBO Journal*, *31*(4), 1041–1053.

Cisneros, D. A., Pehau-Arnaudet, G., & Francetic, O. (2012). Heterologous assembly of type IV pili by a type II secretion system reveals the role of minor pilins in assembly initiation. *Molecular Microbiology*, *86*(4), 805–818.

Clackson T., Lowman H. B., (2004). Phage Display – A Practical Approach *Oxford University Press New York*

Clausen, M., Jakovljevic, V., Søgaard-Andersen, L., & Maier, B. (2009). High-Force Generation Is a Conserved Property of Type IV Pilus Systems. *Journal of Bacteriology*, *191*(14), 4633–4638.

Collins, R. F., Frye, S. A., Kitmitto, A., Ford, R. C., Tønjum, T., & Derrick, J. P. (2004). Structure of the Neisseria meningitidis Outer Membrane PilQ Secretin Complex at 12 Å Resolution. *Journal of Biological Chemistry*, *279*(38), 39750–39756.

Craig, L., & Li, J. (2008). Type IV pili: paradoxes in form and function. *Current Opinion in Structural Biology*, *18*(2), 267–277.

Craig, L., Pique, M. E., & Tainer, J. A. (2004). Type IV pilus structure and bacterial pathogenicity. *Nature Reviews Microbiology*, *2*(5), 363–378.

Craig, L., Volkmann, N., Arvai, A. S., Pique, M. E., Yeager, M., Egelman, E. H., & Tainer, J. A. (2006). Type IV pilus structure by cryo-electron microscopy and crystallography: Implications for pilus assembly and functions. *Molecular Cell*, *23*(5), 651–662.

Crissman, J. W., & Smith, G. P. (1984). Gene-III protein of filamentous phages: Evidence for a carboxyl-terminal domain with a role in morphogenesis. *Virology*, *132*(2), 445–455.

Davis, B. M., Lawson, E. H., Sandkvist, M., Ali, A., Sozhamannan, S., & Waldor, M. K. (2000). Convergence of the secretory pathways for cholera toxin and the filamentous phage, CTXϕ. *Science*, *288*(5464), 333–335.

Davis, B. M., & Waldor, M. K. (2000). CTXφ contains a hybrid genome derived from tandemly integrated elements. *Proceedings of the National Academy of Sciences*, *97*(15), 8572–8577.

Deng, L.-W., Malik, P., & Perham, R. N. (1999). Interaction of the globular domains of pIII protein of filamentous bacteriophage fd with the F-pilus of *Escherichia coli*. *Virology*, *253*(2), 271–277.

Deng, L.-W., & Perham, R. N. (2002). Delineating the site of interaction on the pIII protein of filamentous bacteriophage fd with the F-pilus of *Escherichia coli. Journal of Molecular Biology*, *319*(3), 603–614.

DiRita, V. J. (1992). Co-ordinate expression of virulence genes by ToxR in *Vibrio cholerae. Molecular Microbiology*, *6*(4), 451–458.

DiRita, V. J., Parsot, C., Jander, G., & Mekalanos, J. J. (1991). Regulatory cascade controls virulence in *Vibrio cholerae*. *Proceedings of the National Academy of Sciences of the United States of America*, *88*(12), 5403–5407.

Durand, É., Michel, G., Voulhoux, R., Kürner, J., Bernadac, A., & Filloux, A. (2005). XcpX controls biogenesis of the *Pseudomonas aeruginosa* XcpT-containing Pseudopilus. *Journal of Biological Chemistry*, *280*(36), 31378–31389.

Dziejman, M., Balon, E., Boyd, D., Fraser, C. M., Heidelberg, J. F., & Mekalanos, J. J. (2002). Comparative genomic analysis of *Vibrio cholerae*: Genes that correlate with cholera endemic and pandemic disease. *Proceedings of the National Academy of Sciences*, *99*(3), 1556–1561.

Field, M. (1977). New strategies for treating watery diarrhea. *New England Journal of Medicine*, *297*(20), 1121–1122.

Ford, C. G., Kolappan, S., Phan, H. T. H., Waldor, M. K., Winther-Larsen, H. C., & Craig, L. (2012). Crystal structures of a CTXφ pIII domain unbound and in complex with a *Vibrio cholerae* TolA domain reveal novel interaction Interfaces. *The Journal of Biological Chemistry*, *287*(43), 36258–36272.

Giltner, C. L., Habash, M., & Burrows, L. L. (2010). *Pseudomonas aeruginosa* minor pilins are incorporated into Type IV pili. *Journal of Molecular Biology*, *398*(3), 444–461.

Giltner, C. L., Rana, N., Lunardo, M. N., Hussain, A. Q., & Burrows, L. L. (2011). Evolutionary and functional diversity of the *Pseudomonas* type IVa pilin island. *Environmental Microbiology*, *13*(1), 250–264.

Girón, J. A., Levine, M. M., & Kaper, J. B. (1994). Longus: a long pilus ultrastructure produced by human enterotoxigenic *Escherichia coli*. *Molecular Microbiology*, *12*(1), 71–82.

Goodman, B. E., & Percy, W. H. (2005). CFTR in cystic fibrosis and cholera: from membrane transport to clinical practice. *Advances in Physiology Education*, *29*(2), 75–82.

Gurung, I., Spielman, I., Davies, M. R., Lala, R., Gaustad, P., Biais, N., & Pelicic, V. (2016). Functional analysis of an unusual type IV pilus in the Gram-positive *Streptococcus sanguinis*. *Molecular Microbiology*, *99*(2), 380–392.

Häse, C. C., & Mekalanos, J. J. (1998). TcpP protein is a positive regulator of virulence gene expression in Vibrio cholerae. *Proceedings of the National Academy of Sciences*, *95*(2), 730–734.

Heilpern, A. J., & Waldor, M. K. (2000). CTXφ infection of *Vibrio cholerae* requires the tolQRA gene products. *Journal of Bacteriology*, *182*(6), 1739–1747.

Heilpern, A. J., & Waldor, M. K. (2003). pIIICTX, a predicted CTXφ Minor Coat Protein, can expand the host range of coliphage fd to include *Vibrio cholerae*. *Journal of Bacteriology*, *185*(3), 1037–1044.

Helaine, S., Dyer, D. H., Nassif, X., Pelicic, V., & Forest, K. T. (2007). 3D structure/function analysis of PilX reveals how minor pilins can modulate the virulence properties of type IV pili. *Proceedings of the National Academy of Sciences*, *104*(40), 15888–15893.

Higa, N., Honma, Y., Albert, M. J., & Iwanaga, M. (1993). Characterization of *Vibrio cholerae* O139 synonym Bengal isolated from patients with cholera-like disease in Bangladesh. *Microbiology and Immunology*, *37*(12), 971–974.

Holliger, P., Riechmann, L., & Williams, R. L. (1999). Crystal structure of the two N-terminal domains of g3p from filamentous phage fd at 1.9 Å: evidence for conformational lability. *Journal of Molecular Biology*, *288*(4), 649–657.

Horiuchi, T., & Komano, T. (1998). Mutational analysis of plasmid R64 thin pilus prepilin: the entire prepilin sequence is required for processing by Type IV prepilin Peptidase. *Journal of Bacteriology*, *180*(17), 4613–4620.

Huber, K. E., & Waldor, M. K. (2002). Filamentous phage integration requires the host recombinases XerC and XerD. *Nature*, *417*(6889), 656–659.

Imhaus, A.-F., & Duménil, G. (2014). The number of *Neisseria meningitidis* type IV pili determines host cell interaction. *The EMBO Journal*, *33*(16), 1767–1783.

Kaya B. K., Kurakin A. V., Hyde-DeRuyscher R., (1998) From peptides to drugs via phage display. *Drug Discovery Today* 3: 370–378

Kaper, J. B., Morris, J. G., & Levine, M. M. (1995). Cholera. *Clinical Microbiology Reviews*, *8*(1), 48–86.

Karaolis, D. K. R., Johnson, J. A., Bailey, C. C., Boedeker, E. C., Kaper, J. B., & Reeves, P. R. (1998). A *Vibrio cholerae* pathogenicity island associated with epidemic and pandemic strains. *Proceedings of the National Academy of Sciences*, *95*(6), 3134–3139.

Karlsson, F., Borrebaeck, C. A. K., Nilsson, N., & Malmborg-Hager, A.-C. (2003). The mechanism of bacterial infection by filamentous phages involves molecular interactions between TolA and phage protein 3 domains. *Journal of Bacteriology*, *185*(8), 2628–2634.

Karuppiah, V., Thistlethwaite, A., & Derrick, J. P. (2016). Structures of type IV pilins from *Thermus thermophilus* demonstrate similarities with type II secretion system pseudopilins. *Journal of Structural Biology*, *196*(3), 375–384.

Kirn, T. J., Bose, N., & Taylor, R. K. (2003). Secretion of a soluble colonization factor by the TCP type 4 pilus biogenesis pathway in *Vibrio cholerae*. *Molecular Microbiology*, *49*(1), 81–92.

Kirn, T. J., Lafferty, M. J., Sandoe, C. M. P., & Taylor, R. K. (2000). Delineation of pilin domains required for bacterial association into microcolonies and intestinal colonization by Vibrio cholerae. *Molecular Microbiology*, *35*(4), 896–910.

Kolappan, S., Coureuil, M., Yu, X., Nassif, X., Egelman, E. H., & Craig, L. (2016). Structure of the *Neisseria meningitidis* Type IV pilus. *Nature Communications*, *7*.

Kolappan, S., Ng, D., Yang, G., Harn, T., & Craig, L. (2015). Crystal structure of the minor pilin CofB, the initiator of CFA/III pilus assembly in Enterotoxigenic *Escherichia coli*. *Journal of Biological Chemistry*, *290*(43), 25805–25818.

Korotkov, K. V., & Hol, W. G. J. (2008). Structure of the GspK–GspI–GspJ complex from the enterotoxigenic *Escherichia coli* type 2 secretion system. *Nature Structural & Molecular Biology*, *15*(5), 462–468.

Korotkov, K. V., & Hol, W. G. J. (2013). Crystal structure of the pilotin from the enterohemorrhagic *Escherichia coli* type II secretion system. *Journal of Structural Biology*, *182*(2), 186–191.

Korotkov, K. V., Johnson, T. L., Jobling, M. G., Pruneda, J., Pardon, E., Héroux, A., … Hol, W. G. J. (2011). Structural and Functional Studies on the Interaction of GspC and GspD in the Type II Secretion System. *PLOS Pathogens*, *7*(9), e1002228.

Korotkov, K. V., Sandkvist, M., & Hol, W. G. J. (2012). The type II secretion system: biogenesis, molecular architecture and mechanism. *Nature Reviews. Microbiology*, *10*(5), 336–351.

Kovach, M. E., Shaffer, M. D., & Peterson, K. M. (1996). A putative integrase gene defines the distal end of a large cluster of ToxR-regulated colonization genes in Vibrio cholerae. *Microbiology*, *142*(8), 2165–2174.

Leighton, T. L., Dayalani, N., Sampaleanu, L. M., Howell, P. L., & Burrows, L. L. (2015). Novel role for PilNO in Type IV Pilus retraction revealed by alignment subcomplex mutations. *Journal of Bacteriology*, *197*(13), 2229–2238.

Lemichez E. and Stefani C (2013). Cholera toxin notches epithelial junctions. *Cell host & Microbe.* 14(3), 294-305.

Lencer, W. I., & Tsai, B. (2003). The intracellular voyage of cholera toxin: going retro. *Trends in Biochemical Sciences*, *28*(12), 639–645.

Levine, M. M., Kaper, J. B., Black, R. E., & Clements, M. L. (1983). New knowledge on pathogenesis of bacterial enteric infections as applied to vaccine development. *Microbiological Reviews*, *47*(4), 510–550.

Levistre, R., Berguerand, M., Bereziat, G., & Masliah, J. (1995). The cross-regulation of G_i-protein by cholera toxin involves a phosphorylation by protein kinase A. *Biochemical Journal*, *306*(3), 765–769.

Li, J., Egelman, E. H., & Craig, L. (2012). Structure of the *Vibrio cholerae* Type IVb pilus and stability comparison with the *Neisseria gonorrheae* Type IVa pilus. *Journal of Molecular Biology*, *418*(1–2), 47–64.

Lonrroth, I. & Holmgren, J. (1973). Subunit structure of cholera toxin. *Microbiology*, *76*(2), 417–427.

Lospalluto, J., & Finkelstein, R. (1972). Chemical and physical properties of cholera exo-enterotoxin (choleragen) and its spontaneously formed toxoid (choleragenoid). *Biochimica et Biophysica Acta (BBA) - Protein Structure*, *257*(1), 158–166.

Lubkowski, J., Hennecke, F., Plückthun, A., & Wlodawer, A. (1999). Filamentous phage infection: crystal structure of g3p in complex with its coreceptor, the C-terminal domain of TolA. *Structure*, *7*(6), 711–722.

Maier, B., Potter, L., So, M., Seifert, H. S., & Sheetz, M. P. (2002). Single pilus motor forces exceed 100 pN. *Proceedings of the National Academy of Sciences of the United States of America*, *99*(25), 16012–16017.

Maier, B., & Wong, G. C. L. (2015). How bacteria use Type IV pili machinery on surfaces. *Trends in Microbiology*, *23*(12), 775–788.

Mazariego-Espinosa, K., Cruz, A., Ledesma, M. A., Ochoa, S. A., & Xicohtencatl-Cortes, J. (2010). Longus, a Type IV pilus of Enterotoxigenic *Escherichia coli,* is involved in adherence to intestinal epithelial cells. *Journal of Bacteriology*, *192*(11), 2791–2800.

Megli, C. J., & Taylor, R. K. (2013). Secretion of TcpF by the *Vibrio cholerae* toxin-coregulated pilus biogenesis apparatus requires an N-terminal determinant. *Journal of Bacteriology*, *195*(12), 2718–2727.

Melville, S., & Craig, L. (2013). Type IV pili in Gram-positive bacteria. *Microbiology and Molecular Biology Reviews: MMBR*, *77*(3), 323–341.

Merz, A. J., So, M., & Sheetz, M. P. (2000). Pilus retraction powers bacterial twitching motility. *Nature*, *407*(6800), 98–102.

Ng, D., Harn, T., Altindal, T., Kolappan, S., Marles, J. M., Lala, R., … Craig, L. (2016). The *Vibrio cholerae* minor pilin TcpB initiates assembly and retraction of the toxin-coregulated pilus. *PLoS Pathogens*, 12(12): e1006109

Nguyen, Y., Harvey, H., Sugiman-Marangos, S., Bell, S. D., Buensuceso, R. N. C., Junop, M. S., & Burrows, L. L. (2015). Structural and functional studies of the *Pseudomonas aeruginosa* minor pilin, PilE. *Journal of Biological Chemistry*, *290*(44), 26856–26865.

Nguyen, Y., Sugiman-Marangos, S., Harvey, H., Bell, S. D., Charlton, C. L., Junop, M. S., & Burrows, L. L. (2015). Pseudomonas aeruginosa minor pilins prime Type IVa pilus assembly and promote surface display of the PilY1 adhesin. *Journal of Biological Chemistry*, *290*(1), 601–611.

Ochman, H., Lawrence, J. G., & Groisman, E. A. (2000). Lateral gene transfer and the nature of bacterial innovation. *Nature*, *405*(6784), 299–304.

Pasloske, B. L., & Paranchych, W. (1988). The expression of mutant pilins in Pseudomonas aeruginosa: fifth position glutamate affects pilin methylation. *Molecular Microbiology*, *2*(4), 489–495.

Pearson, G. D., Woods, A., Chiang, S. L., & Mekalanos, J. J. (1993). CTX genetic element encodes a site-specific recombination system and an intestinal colonization factor. *Proceedings of the National Academy of Sciences*, *90*(8), 3750–3754.

Pollastri, G., & McLysaght, A. (2005). Porter: a new, accurate server for protein secondary structure prediction. *Bioinformatics*, *21*(8), 1719–1720.

Pollitzer, W. S., Chernoff, A. I., Horton, L. L., & Froehlich, M. (1959). Hemoglobin patterns in American Indians. *Science*, *129*(3343), 216–216.

Reichow, S. L., Korotkov, K. V. Hol, W.G.J., Gonen. T. (2010) *Structure of the cholera toxin secretion channel in its closed state* Nature Structure Mol. Biol., 17 1226-1232.

Riechmann, L., & Holliger, P. (1997). The C-Terminal Domain of TolA Is the coreceptor for filamentous phage infection of *E. coli*. *Cell*, *90*(2), 351–360.

Russel, M. (1998). Macromolecular assembly and secretion across the bacterial cell envelope: type II protein secretion systems11Edited by P. E. Wright. *Journal of Molecular Biology*, *279*(3), 485–499.

Sandkvist, M. (2001). Biology of type II secretion. *Molecular Microbiology*, *40*(2), 271–283.

Sandkvist, M., Michel, L. O., Hough, L. P., Morales, V. M., Bagdasarian, M., Koomey, M., … Bagdasarian, M. (1997). General secretion pathway (eps) genes required

for toxin secretion and outer membrane biogenesis in *Vibrio cholerae*. *Journal of Bacteriology*, *179*(22), 6994–7003.
Sauvonnet, N., Vignon, G., Pugsley, A. P., & Gounon, P. (2000). Pilus formation and protein secretion by the same machinery in *Escherichia coli*. *The EMBO Journal*, *19*(10), 2221–2228.
Silhavy, T. J., Kahne, D., & Walker, S. (2010). The Bacterial Cell Envelope. *Cold Spring Harbor Perspectives in Biology*, *2*(5).
Skerker, J. M., & Berg, H. C. (2001). Direct observation of extension and retraction of type IV pili. *Proceedings of the National Academy of Sciences*, *98*(12), 6901–6904.
Stengele, I., Bross, P., Garces, X., Giray, J., & Rasched, I. (1990). Dissection of functional domains in phage fd adsorption protein. *Journal of Molecular Biology*, *212*(1), 143–149.
Stone, K. D., Hong-Zhong Z., Carlson L. K. & Donnenberg, M.S. (1996). A cluster of fourteen genes from enteropathogenic *Escherichia coli* is sufficient for the biogenesis of a type IV pilus. *Molecular Microbiology*. 20(2) 325-337.
Strom M.S, & Lory, S. (1993). Structure-function and biogenesis of the Type IV pili. *Annual Review of Microbiology*, *47*(1), 565–596.
Taylor, R. K., Miller, V. L., Furlong, D. B., & Mekalanos, J. J. (1987). Use of phoA gene fusions to identify a pilus colonization factor coordinately regulated with cholera toxin. *Proceedings of the National Academy of Sciences*, *84*(9), 2833–2837.
Tripathi, S. A., & Taylor, R. K. (2007). Membrane association and multimerization of TcpT, the cognate ATPase ortholog of the *Vibrio cholerae* toxin-coregulated-pilus biogenesis apparatus. *Journal of Bacteriology*, *189*(12), 4401–4409.
van Heyningen, S. (1976). The subunits of cholera toxin: Structure, stoichiometry, and function. *The Journal of Infectious Diseases*, *133*(Supplement_1), S5–S13.
Vezzulli, L., Grande, C., Reid, P. C., Hélaouët, P., Edwards, M., Höfle, M. G., … Pruzzo, C. (2016). Climate influence on *Vibrio* and associated human diseases during the past half-century in the coastal North Atlantic. *Proceedings of the National Academy of Sciences*, *113*(34), E5062–E5071.
Waldor, M. K., Colwell, R., & Mekalanos, J. J. (1994). The *Vibrio cholerae* O139 serogroup antigen includes an O-antigen capsule and lipopolysaccharide virulence determinants. *Proceedings of the National Academy of Sciences*, *91*(24), 11388–11392.
Waldor, M. K. & Friedman D. I. (2005). Phage regulatory circuits and virulence gene expression. *Current Opinion in Microbiology*. 8(4), 459-465.
Waldor M. K., & Mekalanos, J. J. (1996). Lysogenic conversion by a filamentous phage encoding cholera toxin. *Science*. 272(5270), 1910-1914.
Wall, D., & Kaiser, D. (1999). Type IV pili and cell motility. *Molecular Microbiology*, *32*(1), 01-10.
Wilke, M. S., Lovering, A. L., & Strynadka, N. C. (2005). β-Lactam antibiotic resistance: a current structural perspective. *Current Opinion in Microbiology*, *8*(5), 525–533.
World Health Organization (WHO). 2013. “Diarrhoeal disease – Fact sheet N°330” *WHO*. 1-4.
World Health Organization (WHO). 2016. “Weekly Epidemiology Record” *WHO*. 38(91):433-440

World Health Organization (WHO). 2017. "WHO publishes list of bacteria for which new antibiotics are urgently needed". Web. June, 2017.

Winther-Larsen, H. C., Wolfgang, M., Dunham, S., Van Putten, J. P. M., Dorward, D., Løvold, C., … Koomey, M. (2005). A conserved set of pilin-like molecules controls type IV pilus dynamics and organelle-associated functions in *Neisseria gonorrhoeae*. *Molecular Microbiology*, *56*(4), 903–917.

Wolfgang, M., Park, H.-S., Hayes, S. F., Putten, J. P. M. van, & Koomey, M. (1998). Suppression of an absolute defect in Type IV pilus biogenesis by loss-of-function mutations in pilT, a twitching motility gene in *Neisseria gonorrhoeae*. *Proceedings of the National Academy of Sciences*, *95*(25), 14973–14978.

Yamagata, H., Taguchi, N., Daishima, K., & Mizushima, S. (1983). Genetic characterization of a gene for prolipoprotein signal peptidase in *Escherichia coli*. *Molecular and General Genetics MGG*, *192*(1–2), 10–14.

Yan, Z. Yin, M. Xu, D. Zhu, Y. & Li, X. (2017). Structural insights into the secretin translocation channel in the type II secretion system. *Nature structural & Molecular Biology* 24, 177-183.

Yuen, A. S. W., Kolappan, S., Ng, D., & Craig, L. (2013). Structure and secretion of CofJ, a putative colonization factor of enterotoxigenic *Escherichia coli*. *Molecular Microbiology*, *90*(4), 898–918.

Zaburdaev, V., Biais, N., Schmiedeberg, M., Eriksson, J., Jonsson, A.-B., Sheetz, M. P., & Weitz, D. A. (2014). Uncovering the mechanism of trapping and cell orientation during *Neisseria gonorrhoeae* twitching motility. *Biophysical Journal*, *107*(7), 1523–1531.